PHYSICAL REVIEW B VOLUME 11, NUMBER 3 1 FEBRUARY 1975

Theory of critical point scattering and correlations. III. The Ising model below T_c and in a field

Howard B. Tarko and Michael E. Fisher*

Baker Laboratory and Materials Science Center, Cornell University, Ithaca, New York 14850

(Received 11 June 1974)

Power-series expansions of the spin-pair correlation functions of the square, sc, and bcc Ising lattices have been obtained using the semi-invariant approach for general field H and temperature T. In three dimensions Páde-approximant analyses indicate $2\nu' = 1.285 \pm 0.020$, in agreement with scaling, but $2\nu^c \simeq 0.835 \pm 0.02$ which is some (1–3)% above the scaling prediction $\nu^c = \nu/\beta\delta \simeq 0.823$. However, ratio techniques reveal that this discrepancy can be attributed to significant confluent critical singularities. Cubic and quintic parametric representations of the critical equation of state, and corresponding expressions for the correlation length, $\xi_1(H,T)$, are developed, which are considerable improvements over the linear model. The universality and spherical symmetry of the critical scattering intensity $\hat{\chi}(\vec{k},H,T)$ is confirmed to within (1–2)% by estimating suitable invariant combinations of amplitudes. The deviations from Ornstein-Zernike theory for general H and T are found to be considerably greater than for $H=0$, $T>T_c$. Complete parametric scaling representations of $\hat{\chi}(\vec{k},H,T)$ are developed for three dimensions; corresponding scaling approximants are constructed in two dimensions but only for $T=T_c$ and for $T \gtrless T_c$ with $H=0$.

I. INTRODUCTION

As one approaches the critical point of many systems a dramatic increase in the scattering cross section in certain directions is observed. For a ferromagnet this critical scattering can be seen most readily in scattering experiments performed with neutrons; the small-angle scattering in the vicinity of the critical point increases sharply as $T \to T_c$. It is now well established that this phenomenon is due to the divergence of the spatial range of the magnetization fluctuations at the critical point. If the scattering is quasielastic (or can be suitably corrected for inelasticity) one finds (in first Born approximation) that the scattering intensity is proportional to the Fourier transform of the appropriate pair-correlation function.[1-3] For a ferromagnet or fluid, the study of critical scattering thus reduces to an investigation of the behavior of the spin-spin or particle-particle correlations, respectively, in the critical region.

In Paper I of this series,[4] the behavior of the scattering intensity above T_c and in zero magnetic field was analyzed in detail for the spin-$\frac{1}{2}$ Ising-model ferromagnet in dimensions $d=2$ and $d=3$ on the basis of exact series expansions. In the interpretation of the model as a lattice gas or fluid, zero field corresponds to the critical isochore $\rho = \rho_c$; in the interpretation as a binary AB alloy system, zero field corresponds to equal mole fractions of the two components, i.e., $x_a = x_b$. Similar calculations were performed in Paper II[5] for Heisenberg models of general spin (including the classical limit $S \to \infty$) on three-dimensional lattices.

These studies lead to estimates of the exponent ν, describing the divergence of the correlation length $\xi(T, H=0)$, and of the exponent η for the variation of the scattering intensity at the critical point itself. The nonzero values found for η confirmed the failure of the classical, Ornstein-Zernike theory,[6] as anticipated earlier.[2] Similar results were found by Jasnow and Wortis[7] in their work on the $S=\infty$, anisotropic Heisenberg models.

The analyses of I and II also lead to explicit approximants for the scattering intensity as a function of temperature T, and wave number $\vec{k}$. These expressions, in turn, confirm the scaling theory of the critical correlations[2,8] and lead to approximants for the asymptotic scaling functions themselves. Furthermore, the universality of the scaling functions (and the exponents), specifically, their lattice independence (given the dimensionality, d, and number of isotropically coupled spin components, n) is confirmed to within the available numerical precision. However, the scaling theory of the correlations[2,8] also makes definite predictions for the scattering *below* the critical point, and for the scattering as a function of magnetic field (or, in the case of a fluid, as a function of density of chemical-potential deviation). Specifically, the correlation-length exponent below T_c is predicted to satisfy $\nu' = \nu$, while the corresponding exponent for the field dependence at $T = T_c$ should be $\nu^c = \nu/(\beta+\gamma)$, where β and γ are the spontaneous magnetization and susceptibility exponents, respectively.[2] Up to this time essentially none of these predictions have been tested by theoretical work. Furthermore, the theoretical description of the scattering below T_c is already of relevance to experimental work on ferromagnets, antiferromagnets, and binary alloys. With improving experimental techniques the behavior of the scattering as a function of density, as well as temperature, should soon be a focus of work on fluids; scattering experiments on ferromagnets in a finite magnetic field can no doubt be anticipated before too long.

The present paper aims to fill these gaps in theory by studying the spin-spin correlations of the nearest-neighbor spin-$\frac{1}{2}$ Ising model in two and three dimensions as a function of both field H and temperature T. As in parts I and II, our analysis is mainly based on the systematic extrapolation of power-series expansions for various moments of the correlation function, but now in the high-field and low-temperature variables $y=\exp(-2mH/k_BT)$ and $u=\exp(-4J/k_BT)$. Particular attention has been paid to the *phase boundary*, i.e., $H=0+$, $M=M_0(T)$, $T<T_c$ [or $\rho=\rho_{\text{liq}}(T)$ or $\rho_{\text{gas}}(T)$ for the fluid picture], and to the *critical isotherm* $T=T_c$. However, with the aid of scaling concepts (which are tested in the analysis) expressions have been developed for the scattering intensity through the whole critical region of the (H, T) plane. Some of our results have been summarized previously in a short communication.[9]

We have derived series for the square and simple-cubic lattices to order y^7, and for the body-centered-cubic lattice to order y^6. Independent calculations for the fcc lattice (to order y^6) have been undertaken by Ritchie.[10] The low-temperature expansions for the moments, etc., to order u^6 for square, u^{11} for sc, and u^{13} for bcc, turn out to be not so well behaved as those on the *critical isochore*, $H=0$, $T>T_c$. Thus our estimates of the exponents are less precise than above T_c and the checks of the scaling predictions are not as tight as might be desired. However, the numerical values of various important critical amplitudes are quite well determined (accepting the preferred exponent estimates) and, in particular, we clearly establish that the deviations of the *form* of the scattering intensity (as a function of T and $\vec{k}$) from the Ornstein-Zernike (OZ) predictions are significantly larger below T_c than above. [It was shown in I and II that the OZ approximation to the scaling function above T_c is accurate over a surprizingly large range in the scaling variable $|\vec{k}|/(T-T_c)^{\nu}$.]

In the bulk of this paper we describe the Ising model in the language appropriate to a ferromagnet. The transcription into lattice-gas models, etc., follows as in I. The notation of parts I and II is retained as closely as possible, but a few extensions and modifications are described in Sec. II, below. As in I, the standard approximate theories, namely, mean-field theory,[11] and the Elliott-Marshall-Bethe approximation,[12] are a convenient point of reference and comparison; they are summarized briefly in Sec. III. The predictions of scaling theory are parametric fits to the equation of state, including cubic and quintic models, are discussed in Sec. IV. Similar fits to the correlation length as a function of H and T, and general considerations pertaining to the nature of the full correlation scaling functions are developed in Sec. V. In Sec. VI we describe the methods used to generate the series expansions of the correlation function, and mention other ancillary calculations. The numerical analyses on the phase boundary and on the critical isotherm are presented in Sec. VII; tables are presented of exponent and amplitude estimates for the various moments on all lattices. Explicit approximants for the susceptibility and correlation length on the phase boundary, and critical isotherm and isochore are presented in Appendix B. The various results are summarized in Sec. VIII where, in adddition, explicit scaling and parametric approximants for the total scattering intensity are constructed and discussed.

II. DEFINITIONS AND NOTATION

The notation of I will be followed except where explicitly indicated. The reader is referred to Secs. II and III of that paper for a detailed discussion of the notation and various other relevant features of the Ising model.

A. Model

The model which we discuss is the spin-$\frac{1}{2}$ Ising model in an external magnetic field H with Hamiltonian

$$\mathcal{H}=-\frac{1}{2}\sum_{\vec{R},\vec{R}'} J(\vec{R}-\vec{R}')s_{\vec{R}}s_{\vec{R}'}-mH\sum_{\vec{R}} s_{\vec{R}}, \qquad (2.1)$$

where $s_{\vec{R}}=\pm 1$ is the spin variable at lattice site $\vec{R}$, m is the magnetic moment of a spin, and $J(\vec{R}-\vec{R}')$ is the exchange integral coupling the spins at $\vec{R}$ and $\vec{R}'$. The sums, $\sum_{\vec{R}}$ run over all lattice sites. In this paper only nearest-neighbor ferromagnetic, $J(\vec{R})>0$, interactions are considered. If $\vec{\delta}$ denotes a nearest-neighbor vector of the lattice, we thus set $J(\vec{\delta})=J$ and $J(\vec{R}-\vec{R}')=0$ if $\vec{R}-\vec{R}\neq\vec{\delta}$. By changing the sign of J our results will describe an *anti*-ferromagnet in a staggered field $H'=H$. (See Sec. 3.1 in I.)

The behavior of the Ising model as a function of magnetic field and temperature can most conveniently be described by the variables

$$K=J/k_BT,\quad L=mH/k_BT,\quad u=x^2=e^{-4K},\quad y=e^{-2L}, \tag{2.2}$$

which enter directly as Boltzmann factors on overturning spins from the fully aligned ground state.

In the critical region we will use the reduced variables

$$t=(T/T_c)-1 \quad\text{and}\quad h=mH/k_BT_c. \tag{2.3}$$

B. Correlation functions and scattering

We will be concerned with the spin-pair correlation function, defined by

$$\Gamma(\vec{R};H,T)=\langle s_{\vec{0}}s_{\vec{R}}\rangle-\langle s_{\vec{0}}\rangle\langle s_{\vec{R}}\rangle, \tag{2.4}$$

where $\langle\ \rangle$ denotes a thermal average, and $s_{\vec{0}}$ is the spin at an arbitrary origin. It should be noted that this definition of Γ differs from that in I by a factor $(1-\langle s_{\vec{0}}\rangle\langle s_{\vec{R}}\rangle)$. If radiation of wave vector $\vec{k}_0$ is scattered elastically, yielding a final wave vector $\vec{k}_f$, with $|\vec{k}_0|=|\vec{k}_f|$, then the scattering intensity $I(\vec{k})$ is a function of the transfer wave vector, $\vec{k}=\vec{k}_f-\vec{k}_0$ and is given in Born approximation by

$$I(\vec{k})/I_0(\vec{k})=\hat{\chi}(\vec{k})=\hat{\Gamma}(\vec{k}), \tag{2.5}$$

where the Fourier transform is defined by

$$\hat{\Gamma}(\vec{k},H,T)=\sum_{\vec{R}}e^{i\vec{k}\cdot\vec{R}}\Gamma(\vec{R},H,T), \tag{2.6}$$

and $I_0(\vec{k})$ is the corresponding scattering intensity from the equivalent set of noninteracting spins. [In contrast to I, where $\hat{\chi}(\vec{k})=1+\hat{\Gamma}(\vec{k})$, the definitions of $\hat{\Gamma}(\vec{k})$ and $\hat{\chi}(\vec{k})$ have been chosen to coincide; in the subsequent discussion $\hat{\chi}(\vec{k})$ and $\hat{\Gamma}(\vec{k})$ will be used interchangeably.] For the purpose of calculation it is convenient to define explicitly an inverse correlation function $\mathcal{C}(\vec{R},H,T)$ with Fourier transform

$$\hat{\mathcal{C}}(\vec{k},H,T)=\sum_{\vec{r}}e^{i\vec{k}\cdot\vec{R}}\mathcal{C}(\vec{R},H,T) \tag{2.7}$$

defined through

$$\hat{\mathcal{C}}(\vec{k})=1/\hat{\Gamma}(\vec{k}). \tag{2.8}$$

Clearly, $\mathcal{C}(\vec{R})$ is closely related to the direct correlation function, $C(\vec{R})$, defined originally by Ornstein and Zernike.[6]

C. Moments and the correlation length

Away from the critical point the reduced scattering intensity, $\hat{\chi}(\vec{k})$, can be expanded about $\vec{k}=0$ in the form

$$\hat{\chi}(0)/\hat{\chi}(\vec{k})=1+\Lambda_2(H,T)k^2a^2+O(k^4a^4), \tag{2.9}$$

where

$$\Lambda_2(H,T)=(\xi_1a)^2=\frac{1}{(\kappa_1a)^2}=\frac{d\ln\hat{\Gamma}(\vec{k})}{d(k^2a^2)}\bigg|_{k=0}. \tag{2.10}$$

This defines $\xi_1(H,T)=1/\kappa_1$ as the effective range of correlation or the *second moment correlation length*. The function $\Lambda_2(H,T)$ can be conveniently expressed in terms of the spherical moments of the correlation function, namely,

$$\mu_l(H,T)=\sum_{\vec{R}}(R/a)^l\Gamma(\vec{R},H,T). \tag{2.11}$$

Then we have

$$\Lambda_2(H,T)=\mu_2(H,T)/2d\mu_0(H,T), \tag{2.12}$$

where d is the dimensionality of the lattice. [Again, a slight difference in notation from I should be noted.] By the fluctuation theorem, the reduced static susceptibility is given by

$$\begin{aligned}\chi_0(H,T)&=(k_BT/m^2)\chi_T(H,T)\\&=(k_BT/m)(\partial M/\partial H)_T=\mu_0(H,T),\end{aligned} \tag{2.13}$$

where $M=\langle s_0\rangle$ is the reduced magnetization per site. [The corresponding relation in I was $\chi_0(T)=1+\mu_0(T)$.]

D. True range of correlation

The "true" or exponential range of correlation, $\xi_{\vec{e}}=1/\kappa_{\vec{e}}$, in the direction $\vec{e}$ is defined by

$$1/\xi_{\vec{e}}=\kappa_{\vec{e}}=-\lim_{\vec{R}\to\infty}R^{-1}\ln|\Gamma(R\vec{e})|, \tag{2.14}$$

which implies that for large R the correlation function decays as $\exp(-\kappa_{\vec{e}}R)$ in the direction of the unit vector $\vec{e}$. It follows immediately that $\kappa_{\vec{e}}$ will be determined by the pole (or the more general singularity) of $\hat{\Gamma}(k\vec{e})$ closest to the real axis in the complex k plane, which must be located at $k=\pm i\kappa_{\vec{e}}$.

Rather than work directly with $\kappa_{\vec{e}}$ or $\exp(-\kappa_{\vec{e}}a)$ it is usually more convenient (see I) to define the coefficient

$$\Lambda_2'(\kappa_{\vec{e}}a)=f^2/2[\cosh(f\kappa_{\vec{e}}a)-1], \tag{2.15}$$

where f is a geometric factor which depends on $\vec{e}$ and the lattice considered. For a tabulation of factors f for various directions $\vec{e}$ and for different lattices, and for a more detailed discussion of Λ_2' and $\kappa_{\vec{e}}$, the reader is referred to I. In the case of Ornstein-Zernike theory, Λ_2' and Λ_2 are identical, so that the difference $(\Lambda_2'-\Lambda_2)$ provides a direct measure of the departure of a given system from OZ theory. Near the critical point we expect the correlation function to be spherically symmetric and this will be checked explicitly. With this in mind we drop the subscript $\vec{e}$ from the true range of correlation, $\xi_{\vec{e}}$, denoting it by $\xi=1/\kappa$.

E. Critical exponents and amplitudes

At the critical point the expansion (2.9) fails because the effective range of correlation, and hence Λ_2, becomes infinite as do all the moments μ_l. The correlation function behaves as

$$\hat{\Gamma}(\vec{k}, 0, T_c) = \hat{\Gamma}_c(\vec{k}) \approx \hat{D}/(ka)^{2-\eta}, \tag{2.16}$$

while in real space the correlation function becomes long range, behaving as

$$\Gamma(\vec{R}, 0, T_c) = \Gamma_c(\vec{R}) \approx D/(R/a)^{d-2+\eta},$$
$$T = T_c, \quad H = 0, \quad R \to \infty. \tag{2.17}$$

These relations, of course, serve to define the exponent η. The asymptotic behavior of $\kappa_{e}^{-}a$, $\kappa_1 a$, and μ_l in the vicinity of the critical point depends on how the critical point is approached; we will consider in detail the three loci.

(a) Critical isochore: $H=0, T>T_c$, where the exponents ν, ν_1, and ν_p and corresponding amplitudes are defined as $t\to 0+$ by

$$\xi(T)/a = 1/\kappa a \approx f^+ t^{-\nu},$$
$$\xi_1(T)/a = 1/\kappa_1 a \approx f_1^+ t^{-\nu_1}, \tag{2.18}$$

$$\chi_0(T) \approx C^+ t^{-\gamma},$$
$$\mu_{2p}(T) \approx m_p^+ t^{-2p\nu_p-\gamma}, \tag{2.19}$$

where t was defined in (2.3). (Note that in I the amplitudes $F=1/f^+$ and $F_1 = 1/f_1^+$ were employed.)

(b) Phase boundary: $H=0+, T<T_c$. As $t\to 0-$ we similarly define ν' and f^- by

$$\xi(T)/a = 1/\kappa a \approx f^-(-t)^{-\nu'}, \tag{2.20}$$

with analogous definitions of ν_p', f_1^-, C^-, and m_p^- in which γ' replaces γ. We also define the amplitude and exponent of the spontaneous magnetization by[2]

$$M_0(T) = \lim_{H\to 0+} \langle s_0 \rangle \approx B(-t)^{\beta}. \tag{2.21}$$

(c) Critical isotherm: $T=T_c, H>0$. Finally, exponents ν^c, ν_1^c, and ν_p^c and corresponding amplitudes are defined, as $H\to 0$, by

$$\xi(H)/a = 1/\kappa a \approx f^c |h|^{-\nu^c},$$
$$\xi_1(H)/a \approx f_1^c |h|^{-\nu_1^c}, \tag{2.22}$$

$$\chi_0(H) \approx C^c |h|^{-\gamma^c},$$
$$\mu_{2p}(H) \approx m_p^c |h|^{-2p\nu_p^c-\gamma^c}, \tag{2.23}$$

where, using standard exponent notation,[2] we have

$$\gamma^c = (\delta-1)/\delta. \tag{2.24}$$

Now the homogeneity and scaling hypotheses[2,8] predict, in the first place, that

$$\gamma = \gamma' = \beta(\delta-1) = \beta\delta\gamma^c = (\beta+\gamma)\gamma^c, \tag{2.25}$$

and second, for the correlations

$$\gamma = (2-\eta)\nu \quad \text{with } \nu = \nu_1 = \nu_p \quad (p \geq 1). \tag{2.26}$$

These correlation relations were tested in I and found to hold to within the fairly high precision apparently available. Similarly, we expect

$$\nu' = \nu_1' = \nu_p' \quad \text{and} \quad \nu^c = \nu_1^c = \nu_p^c, \quad (p\geq 1), \tag{2.27}$$

and, more strongly, the scaling hypotheses predict the symmetry relation,

$$\nu' = \nu, \tag{2.28}$$

and, for the critical isotherm,

$$\nu^c = \nu/\beta\delta = \nu/(\beta+\gamma). \tag{2.29}$$

An important aim of our work was to test these last three relations. In fact, we have found them to be consistent with the available data although it unfortunately transpires that the precision attainable is not as good as might be hoped. In the more detailed analyses to determine critical amplitudes and the scaling functions, we will assume the validity of (2.28) and (2.29).

III. APPROXIMATE THEORIES

As in I it is instructive to examine the basic approximate theories since they yield an informative basis for comparison.

A. Mean-field theory

The general result of mean-field theory is[11]

$$\hat{\chi}(\vec{k}, M, T) = \frac{1-M^2}{1-\hat{J}(\vec{k})(1-M^2)/k_B T}, \tag{3.1}$$

where the Fourier transform of the interactions is

$$\hat{J}(\vec{k}) = \sum_{\vec{R}} e^{i\vec{k}\cdot\vec{R}} J(\vec{R}) = \hat{J}(0)[1 - a^2K^2(\vec{k})/2d]. \tag{3.2}$$

Here the second part introduces the effective wave number $K \approx k[1+O(k^2a^2)]$ as in Eq. (2.2) of I. The reduced magnetization, M, in (3.1) is defined simply by

$$M(H, T) = \langle s_0 \rangle. \tag{3.3}$$

By setting $M\equiv 0$ the critical temperature is found from

$$kT_c = \hat{J}(0), \tag{3.4}$$

and thence the asymptotic equation of state in the critical region may be written

$$h = M(t + \tfrac{1}{3}M^2), \tag{3.5}$$

where, as usual, the appropriate branch of the solution for $M(h,t)$ must be used below T_c.[11] From this it follows that the exponents take their standard classical values $\beta = \frac{1}{2}$, $\gamma = 1$, and $\delta = 3$ [and γ^c

$=\frac{2}{3}$ in (2.23)]. The reduced susceptibility itself may be written

$$\chi_0(H,T)=\frac{(1-M^2)(1+t)}{t+M^2}, \tag{3.6}$$

from which the critical amplitudes C^+, C^-, and C^c follow [see (2.19) and (2.22)]. Finally, (3.1) may be rewritten as

$$\hat{\chi}(\vec{k},H,T)=\chi_0(H,T)/[1+\xi_1^2K^2(k)], \tag{3.7}$$

with the identification of the correlation length via

$$\xi_1^2(H,T)=1/\kappa_1^2=\frac{a^2(1-M^2)}{2d(t+M^2)}. \tag{3.8}$$

In the critical region the factor $(1-M^2)$ may be dropped and we find $\nu=\nu'=\frac{1}{2}$, $\nu^c=\frac{1}{3}$, and $\eta=0$, as is well known. The correlation length amplitudes f_1^+, f_1^-, and f_1^c [see (2.18) *et seq.*] follow easily. The various amplitudes are listed in Table I together with certain characteristic "dimensionless" combinations which are expected to be *universal*, i.e., to depend on dimensionality but not on lattice structure (see Sec. IV). Also listed in the table are the results discussed below for the Elliott-Marshall-Bethe approximation, and the estimates for the Ising model itself found in this paper, and already available.[2b,4,5]

The true, exponential range of correlation can be found from (3.1) or (3.7) by locating the nearest zero of the denominator. We quote only the result

$$\kappa_x a=-\ln\{1+\kappa_1 a[1+\tfrac{1}{4}(\kappa_1 a)^2]^{1/2}+\tfrac{1}{2}(\kappa_1 a)^2\}, \tag{3.9}$$

for the square ($d=2$) and simple-cubic ($d=3$) lattices along an axis; this holds for all H and T. Evidently $\kappa_x/\kappa_1\to 1$ as the critical point is approached by any route. This conclusion follows more generally from (3.7) when $\kappa_1=1/\xi_1\to 0$.

B. Elliott-Marshall-Bethe approximation

The Bethe approximation is of interest because it includes one nontrivial piece of information about the lattice structure, namely, the coordination number q. It is thus exact for a Bethe lattice or infinite Cayley tree.[2b] Elliott and Marshall[12] extended the approximation to discuss the scattering intensity, but only for zero magnetic field. It is straightforward, although fairly tedious to extend their results to nonzero field.[13] To state the result we use the variables x and y defined in (2.2) and define the local molecular field parameter λ by the solution of

$$\lambda(1+\lambda xy)^{q-1}=(x+\lambda y)^{q-1}. \tag{3.10}$$

The equation of state is then given by

$$M=(1-\lambda^2y^2)/(1+2\lambda xy+\lambda^2y^2), \tag{3.11}$$

from which the critical point is, as usual, found

TABLE I. Susceptibility and correlation amplitudes. The various amplitudes are defined in (2.18) to (2.23). The dimensionless parameters are $Q_1=C^c\delta/(B^{\delta-1}C^+)^{1/\delta}$, $Q_2=(C^+/C^c)(f_1^c/f_1^+)^{2-\eta}$, and $Q_3=\hat{D}(f_1^+)^{2-\eta}/C^+$. Data are listed for mean-field (M.F.) theory, for the Elliot-Marshall-Bethe (EMB) approximation, and for the square, triangular, sc, and bcc Ising lattices. For the square Ising lattice C^+ and C^- are known exactly (Ref. 46). The two-dimensional Ising amplitudes f_1^+ follows from I. In three dimensions the amplitudes C^+ are taken from Ref. 38c and represent slight revisions of the values used in I. Accordingly, the values of f_1^+ given in I [as $(F_1^+)^{-1}$] have been rederived using the values of $(r_1/a)_c$ quoted in I (see Sec. 7.8). The amplitudes f_1^- and f_1^c are obtained in Sec. VII, where the value of C^- is also discussed. The spontaneous magnetization amplitudes, B, are taken from Ref. 20. In three dimensions the exponent values adopted are $\beta=\frac{5}{16}$, $\gamma=1\frac{1}{4}$, $\nu=\frac{9}{14}$, and $\eta=\frac{1}{18}$.

	C^+	C^+/C^-	C^c	f_1^+	f_1^-	f_1^+/f_1^-	f_1^c	Q_1	Q_2	Q_3
M.F.										
$d=2$	1	2	0.480 750	0.5	0.353 553	1.414 214	0.346 681	1	1	1
$d=3$	1	2	0.480 750	0.408 208	0.288 675	1.414 214	0.283 064	1	1	1
EMB										
sq	1.442 695	2	0.666 667	0.735 534	0.520 101	1.414 214	0.5	1	1	1
tr	1.233 152	2	0.584 804	0.620 774	0.438 954	1.414 214	0.427 494	1	1	1
sc	1.233 152	2	0.584 804	0.506 860	0.358 404	1.414 214	0.349 047	1	1	1
bcc	1.158 686	2	0.553 218	0.474 658	0.335 634	1.414 214	0.327 979	1	1	1
Ising										
sq	0.962 582	37.693 562	0.070 60 ±0.000 02	0.567 02 ±0.000 05	0.176 ±0.005	3.22 ±0.08	0.233 ±0.004	0.880 23 ±0.000 25	2.88 ±0.02	0.413 77 ±0.000 10
tr	0.9244 ±0.0004	37.33 ±0.45	0.069 38 ±0.000 03	0.525 11 ±0.000 05				0.880 23 ±0.000 30		0.413 84 ±0.000 10
sc	1.0585 ±0.0010	5.06 ±0.08	0.2602 ±0.0020	0.478 26 ±0.000 40	0.244 ±0.001	1.96 ±0.01	0.257 ±0.008	0.897 ±0.007	1.21_6 ± 0.03	0.896 ±0.005
bcc	0.9868 ±0.0030	5.01 ±0.05	0.2498 ±0.0030	0.444 56 ±0.000 40	0.227 ±0.005	1.96 ±0.03	0.242 ±0.010	0.903 ±0.012	1.21_1 ± 0.04	0.902 ±0.004

to be

$$x_c = \exp(-2J/k_BT_c) = 1 - (2/q),$$

or

$$\tanh(J/k_BT) = (q-1)^{-1}. \tag{3.12}$$

Incidentally the equation of state given by (3.10) and (3.11) is found to be exact to order y^3 for loose-packed lattices as $H\to\infty$. For close-packed lattices the term of order y^2 is exact but the y^3 term is only approximate because of the presence of triangles.

The equation of state in the critical region can still be written in the mean-field form (3.5) but with h replaced by

$$2(q-2)^{-1}\{\ln[q/(q-2)]\}^{-1}h,$$

and the factor $\frac{1}{3}$ by

$$\tfrac{2}{3}(q-1)/\{q^2\ln[q/(q-2)]\}.$$

The critical exponents, of course, have the same values. The reduced susceptibility can similarly be written near the critical point as

$$\chi_0(H,T) \simeq \frac{2}{(q-2)\ln[q/(q-2)]} \times\left(\frac{2(q-1)}{q^2\ln[q/(q-2)]}M^2+t\right)^{-1}, \tag{3.13}$$

from which the amplitudes C^+, C^-, etc., presented in Table I follow immediately. Note that we again have $C^+/C^-=2$.

The reduced scattering intensity can be again written in the form (3.7) but with

$$\kappa_1^2(H,T) = \frac{2d}{a^2}\frac{x(1+2xy\lambda+\lambda^2y^2)}{(x+\lambda y)(1+\lambda xy)} \times\left[\frac{x+2\lambda y+\lambda^2xy^2}{q\lambda y(1-x^2)}-1\right]. \tag{3.14}$$

Close to the critical point this is equivalent to (3.8) but with the factor $2d$ replaced by

$$2d(q-2)^2\ln[q/(q-2)]/2(q-1)$$

and M^2 multiplied by the factor

$$2(q-1)/q^2\ln[q/(q-2)].$$

The values of the amplitudes f_1^+, f_1^-, and f_1^c follow as

$$(f_1^+)^2 = 2(f_1^-)^2 = (q-1)/d(q-2)^2\ln[q/(q-2)], \tag{3.15}$$

$$(f_1^c)^3 = q(q-1)/3(2d)^{3/2}(q-2)^2. \tag{3.16}$$

Numerical values are given in Table I. Note in addition that as $q\to\infty$ the results approach the mean-field values. Furthermore the ratio f_1^+/f_1^- is again equal to $\sqrt{2}$ and the combination $Q_2 = (C^+/C^c)(f_1^c/f_1^+)^{2-\eta}$ still has the value unity. These results are to be contrasted with those found for the Ising model in two and three dimensions.

IV. SCALING FOR EQUATION OF STATE

In this section we recapitulate briefly the scaling hypothesis for the equation of state with particular reference to the parametric representations.[14,15] Since the zero-momentum limit of the reduced scattering intensity $\hat{\chi}(\vec{k},H,T)$ is just the static susceptibility, knowledge of the equation of state is pertinent. In particular, we have developed parametric forms for the equation of state sufficiently flexible to accommodate precisely the principal data on the critical isochore isotherm, and on the phase boundary.

A. Scaling hypotheses

According to the scaling or homogeneity hypotheses[2,15] the equation of state $M=\mathfrak{M}(H,T)$ can, when h and t approach zero, be written asymptotically as

$$M \approx |t|^{\beta}B(h/|t|^{\beta\delta}), \tag{4.1}$$

or, equivalently (in the form analyzed by Griffiths[16])

$$h \approx M^{\delta}A(t/M^{1/\beta}). \tag{4.2}$$

By differentiation it follows that the susceptibility can be written similarly, for example,

$$\chi_0 \approx \left(\frac{\partial M}{\partial h}\right)_t \approx |t|^{-\gamma}C^+X(h/|t|^{\beta\delta}). \tag{4.3}$$

For convenience we assume here and below that M and h are never negative; owing to the symmetry about $H=0$ this entails no loss of generality.

The functions $B(z)$ and $X(z)$ have different forms for $t\geq 0$ and $t\leq 0$ but these must match at large arguments.[2] The function $A(w)$ [commonly known as $h(x)$] avoids this matching problem. It has been studied numerically for the Ising model by various authors.[17] Its form in the mean-field approximation where $\delta=3$ and $1/\beta=2$ follows from comparison with (3.5) and is simply

$$A(w) = w^2+\tfrac{1}{3}. \tag{4.4}$$

By rescaling the variables t, h, and M by fixed numerical factors this form can be retained precisely for the Bethe approximation for all q. This "universality" of the scaling function is expected to apply also for the Ising model; i.e., subject only to the parameters which alter exponents, principally the dimensionality d, and the order parameter symmetry n, the scaling functions have fixed forms independent of details of the model.[18] Accordingly, dimensionless combinations such as C^+/C^-, and

$$Q_1 = C^c\delta/(B^{\delta-1}C^+)^{1/\delta} \tag{4.5}$$

should be independent of lattice structure, etc. Evidence supporting this is exhibited in Table I.

B. Parametric representation and linear model

The simple form of scaling function (4.4) cannot apply for more general exponent values ($\gamma \neq 1$, $\beta \neq \frac{1}{2}$), nor can $B(z)$ and $X(z)$ have such explicit forms. This follows from the stringent asymptotic analyticity conditions which the scaling functions must satisfy in the limit of large argument ($w \to \infty$ or $z \to \infty$).[15,16] Accordingly, a parametric representation[14] which automatically ensures the required analyticity properties is more useful.[15] To this end one may introduce a "radial" coordinate $r \geq 0$, which measures the distance in the (H, T) plane from the critical point, and an "angular" coordinate θ, which specifies the corresponding "direction." Conventionally[14,15] one takes $\theta = 0$ on the critical isochore ($H = 0$, $T > T_c$).

For pure power law critical behavior one may then write the scaling hypothesis generally[15] as

$$t \approx rk(\theta), \quad h \approx r^{\beta\delta} l(\theta), \tag{4.6}$$

and

$$M \approx r^{\beta} m(\theta). \tag{4.7}$$

Correspondingly the susceptibility may be written

$$\chi_0 \approx r^{-\gamma} p(\theta), \tag{4.8}$$

where $p(\theta)$ is determined by $k(\theta)$, $l(\theta)$, and $m(\theta)$. With no loss of generality one may choose $k(\theta)$ and $l(\theta)$ to be polynomials; by symmetry the simplest assignment is thus[14]

$$\begin{aligned} k(\theta) &= 1 - b\theta^2 \quad (b > 1), \\ l(\theta) &= l_0\theta(1 - \theta^2). \end{aligned} \tag{4.9}$$

The parameter b fixes the critical isotherm at $\theta_c = b^{-1/2}$.

The so-called *linear model*[14,15] is then specified by

$$m(\theta) = m_0\theta. \tag{4.10}$$

The susceptibility angular function then becomes

$$p(\theta) = p_0\tilde{p}(\theta) \quad \text{with } p_0 = C^+ = m_0/l_0 \tag{4.11}$$

and

$$\tilde{p}(\theta) = \frac{1 - b(1-2\beta)\theta^2}{1 - (3 + b - 2\beta\delta b)\theta^2 + (3 - 2\beta\delta)b\theta^4}. \tag{4.12}$$

If one sets $b = 1 + \frac{1}{3}m_0^2$ and $l_0 = m_0$, the linear model describes the mean-field equation of state, (3.5), exactly. The linear model is also exact to order ϵ^2, with $\epsilon = 4 - d$, for Ising-like models of continuous dimensionality[19] d (although it fails for Heisenberg-like and spherical models owing to the divergence of χ_0 as $H \to 0$ for $T < T_c$ in these models[15,19]).

The two- and three-dimensional Ising models, however, cannot be described in a fully satisfactory way by the linear model. This is seen most directly[17a] by calculating the ratio C^+/C^- from (4.12); the ratio is found to attain a *minimum* value of $(\gamma/\beta)^\gamma[(1-2\beta)/2(\gamma-1)]^{\gamma-1}$ at $b = (\gamma - 2\beta)/\gamma(1-2\beta)$. For the two-dimensional Ising model (with $\beta = \frac{1}{8}$, $\gamma = 1\frac{3}{4}$) this minimum exceeds 60.24; in three dimensions (assuming $\beta = \frac{5}{16}$, $\gamma = 1\frac{1}{4}$) its value is 5.264.[17a] Both these figures significantly exceed the entries in Table I. If, none the less, a "best" linear model is adopted in three dimensions it should have the parameters

$$\begin{aligned} d = 3:\ b = 1\tfrac{1}{3}, \quad & l_0 = 1.0516, \quad m_0 = 1.1131 \quad (\text{sc}), \\ & l_0 = 1.0824, \quad m_0 = 1.0681 \quad (\text{bcc}). \end{aligned} \tag{4.13}$$

Note that the parameters l_0 and m_0 are scale factors which are *not* expected to be universal. The universal dimensionless parameter Q_1 takes the value 0.8936...; unlike the ratio C^+/C^- this does agree moderately well with the estimate in Table I. Despite these defects the linear model works fairly well considering its simplicity. As a test, one may study the derivative amplitudes defined by

$$\left(\frac{\partial^k \chi_0}{\partial h^k}\right)_{t,\,h=0} \approx (k+2)!\,C^+_{(k+2)}\,t^{-\gamma-k\beta\delta}, \tag{4.14}$$

and by the analogous formula for $T < T_c$. These amplitudes have been estimated by Essam and Hunter[20] whose results are shown in Table II. The comparison with the linear model predictions for the sc and bcc lattices are seen to be quite good.

C. Cubic and quintic models

In order to obtain an improved representation of the three-dimensional Ising models and a passable representation of the two-dimensional models it is desirable to extend the linear model. One such extension has been examined by Mulholland and Widom.[21a] They modified the linear model by multiplying both angular functions $l(\theta)$ and $m(\theta)$ in (4.9) and (4.10) by the same factor $(1 - c\theta^2)$. However, this seems unnecessarily complicated as a first step in fitting the equation of state in the (H, T) plane. (Mulholland and Widom were primarily interested in the "unstable" extension of the equation of state into the two phase region and thus chose a form which would ensure van-der-

TABLE II. Tests of parametric equations of state. Susceptibility derivative amplitudes calculated from the linear and cubic models are compared with the results of Essam and Hunter (Ref. 20). Columns (a) give the series estimates of Essam and Hunter for $C^{\pm}_{k+2}$ defined in (4.14) together with the corresponding percentage uncertainties (quoted in parentheses). Columns (b) and (c) show the percentage deviations from the series estimates resulting from the fits to the linear and cubic models, respectively.

	sc			bcc			sq	
	(a)	(b)	(c)	(a)	(b)	(c)	(a)	(c)
C_2^+	0.5299 (0.03)	−0.11	−0.11	0.4952 (0.1)	−0.36	−0.36	0.4812 (0.1)	+0.02
C_4^+	−0.1530 (0.3)	+3.40	−0.26	−0.1385 (1.7)	+1.37	−3.03	−0.1821 (1.2)	+7.03
C_6^+	0.1366 (0.7)	+9.66	+0.07	0.1169 (0.9)	+8.21	−2.82	0.1761 (1.5)	+19.5
C_8^+	−0.1722 (1.4)	+17.5	−0.46	−0.1397 (1.1)	+16.5	−2.93	−0.237 (11)	+32.9
C_{10}^+	0.2601 (3.3)	+25.7	−0.04	0.2023 (3.4)	+23.7	−4.84	0.343 (18)	+62.4
C_{12}^+	−0.453 (12)	+30.0	−4.19	−0.330 (10)	+30	−8.18	−0.731 (17)	+49.1
C_2^-	0.1015 (2.4)	−0.89	+3.65	0.0997 (0.9)	−6.02	−1.60	0.01284 (0.5)	−0.55
C_3^-	−0.0293 (6.8)	−7.85	+4.44	−0.0275 (2.2)	−10.55	+1.09	−0.00291 (1.0)	−6.53
C_4^-	0.0157 (3.8)	−12.10	+10.19	0.0154 (7.1)	−20.1	−1.30	0.00145 (2.1)	−22.8
C_5^-	−0.0115 (7.8)	−18.3	+13.04	−0.0109 (9.2)	−25.7	+2.75	−0.00140 (13)	−56.4
C_6^-	0.0100 (18)	−26.0	+16.0	0.0093 (22)	−32.3	+4.30		

Waals-like "loops" for $\theta > 1$.)

Accordingly, we have investigated two simpler alternatives. The first is a *cubic model* in which the linear form (4.10) is replaced by the cubic

$$m(\theta) = m_0\theta(1 - c\theta^2), \tag{4.15}$$

while (4.9) is retained.[21b] The second is a *quintic model* in which the linear form for $m(\theta)$ and the quadratic form for $k(\theta)$ are kept while the cubic form $l(\theta)$ is extended to a quintic

$$l(\theta) = l_0\theta(1 - \theta^2)(1 - c'\theta^2). \tag{4.16}$$

This last form has the advantage that, with $c' = 1$, it can represent the spherical model exactly for $d = 3$.[15,21c] The corresponding susceptibility angular functions are

cubic:

$$\tilde{p}(\theta) = \frac{1 - (b - 2\beta b + 3c)\theta^2 + bc(3 - 2\beta)\theta^4}{1 - (3 + b - 2\beta\delta b)\theta^2 + (3b - 2\beta\delta b)\theta^4}; \tag{4.17}$$

quintic:

$$\tilde{p}(\theta) = \frac{1 - b(1 - 2\beta)\theta^2}{1 - (3 + b - 2\beta\delta b + 3c')\theta^2 + (3b - 2\beta\delta b + 5c' + 3bc' - 2\beta\delta bc')\theta^4 - bc'(5 - 2\beta\delta)\theta^6}, \tag{4.18}$$

while $p_0 = m_0/l_0 = C^+$ as before.

The cubic model can accommodate the precise estimates for both Q_1 and C^+/C^- in two and in three dimensions. We obtain the fits

$$d = 2: \quad b = 1.2930, \quad c = 0.1853, \tag{4.19}$$

$$d = 3: \quad b = 1.4787, \quad c = 0.06352. \tag{4.20}$$

The corresponding values of the scale factors l_0 and m_0 are listed in Table III. The values of b and c in three dimensions are quite sensitive to C^+/C^- and Q_1. We have adopted the "universal" estimates

$$d = 3: \quad C^+/C^- \simeq 5.03, \quad Q_1 \simeq 0.899, \tag{4.21}$$

which are consistent with data for both bcc and sc. However, for a large range of assigned values of b, both Q_1 and C^+/C^- can be fitted well within the uncertainties by proper choice of c for the cubic model in three dimensions and, to a lesser degree, also in two dimensions. This allows a certain amount of freedom in choosing b, so that one can pick that value which best matches other available data. In fact, we have chosen the values of b and c which reproduce Q_1 and C^+/C^- exactly. By fortunate chance it is found that these values also give the best agreement with the Essam and Hunter estimates of the susceptibility derivative amplitudes as can be seen in Table II. Indeed the agreement in three dimensions is quite remarkable. We should note that in fitting various models

TABLE III. Cubic-model scale parameters l_0 and m_0.

Lattice	l_0	m_0
sq	1.3370	1.2870
sc	1.2574	1.3310
bcc	1.2941	1.2771

we have used amplitude estimates based on series longer than those available to Essam and Hunter. (For references see Table I.) This suggests, in fact, that the error estimates assigned by Essam and Hunter (and shown in Table II) may be somewhat overoptimistic, especially below T_c. Thus, in particular, the values for $C_2^+ = C^+$, $C_2^- = C^-$, and B show deviations from their results. The amplitude fits for the square lattice above T_c are not as precise as in three dimensions but the fits below T_c are surprisingly good.

The quintic model may be similarly analyzed. For three dimensions we find a fit to (4.21) with $b = 1.2889$ and $c' = 0.0473$. Unfortunately, however, no solution can be obtained with the quintic model which represents the data for the two-dimensional lattices. Accordingly, we have restricted ourselves to the cubic model in the subsequent analysis.

V. SCALING OF THE CRITICAL CORRELATIONS

In this section we develop parametric equations for the correlation length $\xi_1(H, T)$ and discuss the scaling theory of the full correlation function.

A. Homogeneity of correlation length

The scaling hypothesis for the correlations is most generally expressed as the asymptotic homogeneity relation[2,8]

$$\hat{\Gamma}(\vec{k}, H, T) \approx \lambda^{2-\eta} \hat{G}(k\lambda, t\lambda^{1/\nu}, h\lambda^{\beta\delta/\nu}), \tag{5.1}$$

as h, t, and k approach zero, where λ is an arbitrary multiplier. The assignment of exponents in (5.1) is dictated by the exponent definitions in Sec. II. Thus if we choose $\lambda = 1/ka$ and let t and h go to zero we obtain the critical point behavior (2.16), with

$$\hat{G}(a^{-1}, 0, 0) = \hat{D}, \tag{5.2}$$

only if the prefactor has the exponent $2 - \eta$.

An expansion of (5.1) in powers of k shows, through (2.10), that the correlation length ξ_1 obeys a scaling relation in the critical region. We may write, in parallel to (4.3),

$$(\xi_1/a)^{-2} = \kappa_1^2 a^2 \approx |t|^{2\nu} y_0 Y(h/|t|^{\beta\delta}),$$
$$y_0 = (f_1^+)^{-2}, \tag{5.3}$$

where again the function $Y(z)$ for $t \geq 0$ and $t \leq 0$ must meet asymptotic conditions as $z \to \infty$ [in order to ensure an analytic variation of ξ_1 with $(T - T_c)$ for $H > 0$]. Alternatively one may introduce the parametric representation

$$[\kappa_1(H, T)a]^2 \approx r^{2\nu} y_0 \tilde{y}(\theta), \tag{5.4}$$

where y_0 is defined in (5.3) and h and t are still given by (4.6). Furthermore, if the polynomial forms (4.7) are employed, one finds that the mean-field results are reproduced exactly by the simple quadratic form

$$\tilde{y}(\theta) = 1 + a_0\theta^2, \tag{5.5}$$

with (4.10), (4.12), and $a_0 = -1 + \frac{2}{3}m_0^2$ and $y_0 = 2d$.

More generally if the quadratic form (4.9) is adopted for $k(\theta)$ and one matches (5.4) on the critical isochore and phase boundary one finds

$$a_0 = (f_1^+/f_1^-)^2(b-1)^{2\nu} - 1. \tag{5.6}$$

The value $b = 1\frac{1}{3}$, appropriate to the "best" linear model for the three-dimensional Ising models, then yields (using Table I) the universal value $a_0 \simeq -0.0644$. This representation can then be checked by calculating f_1^c with the aid of (4.9) and (4.13). One finds $f_1^c \simeq 0.267$ and 0.251 for sc and bcc lattices, respectively, which values lie about 4% above the direct estimates given in Table I (and derived in Sec. VII). Considering the simplicity of the linear model, this agreement is quite gratifying.

As explained in Sec. IV C, the cubic parametric model gives a better fit to the equation of state. Since it utilizes the same quadratic form for $k(\theta)$ the relations (5.6) still apply to (5.5). However, the new values of b given by (4.19) and (4.20) lead to

$$d = 2: \quad a_0 = -0.1099, \tag{5.7}$$

$$d = 3: \quad a_0 = 0.4900. \tag{5.8}$$

These in turn yield new values of the amplitude f_1^c, namely, 0.264, 0.249, and 0.293 for sc, bcc, and square lattices, respectively. These predictions for the three-dimensional lattices are somewhat improved, being about 3% too high. However, the square lattice value is too high by 26%.

In order to obtain a more accurate representation of the available data we have adopted the quartic form

$$\tilde{y}(\theta) = (1 + a_1\theta^2)(1 + a_2\theta^2) \tag{5.9}$$

for use with the cubic model. [See (4.9), (4.15), (4.17), (4.19), (4.20) and Table III.] Fitting now to f_1^+/f_1^- and to the dimensionless ratio

$$Q_2 = (C^+/C^c)(f_1^c/f_1^+)^{2-\eta}, \tag{5.10}$$

for which we adopt the "universal" estimate

$$d=3:\quad Q_2 \simeq 1.21\,, \tag{5.11}$$

(see Table I) leads to the universal parameters

$$\begin{aligned} d=2:&\quad a_1=3.7122,\quad a_2=-0.8111\,,\\ d=3:&\quad a_1=1.1650,\quad a_2=-0.31179\,, \end{aligned} \tag{5.12}$$

while y_0 is still equal to $(f_1^+)^{-2}$. {Incidentally, a [1/1] Padé approximant in θ^2 in place of (5.9), leads to an unacceptable pole in the physical region.} The expression (5.9), is, of course, by no means unique. In principle it could be checked by estimating the derivatives of $\xi_1(H,T)$ with respect to H on the isochore and phase boundary, etc. (as done for the equation of state in Table II). Although we have not undertaken such analyses we believe that the cubic model with (5.9) will provide a reasonable representation of the Ising model correlation length over the whole critical region to an accuracy not significantly less than that of the data utilized.

B. Correlation scaling functions

Starting with the general homogeneity relation (5.1) there are many routes towards the development of scaling forms and, thence, to the calculation of scaling function approximants. Perhaps the simplest conceptually[2c] follows, as before, by putting $\lambda = 1/ka$ which gives

$$\hat{\Gamma}(\vec{k},H,T) \approx \hat{D}(ka)^{-(2-\eta)} Z\left(t/(ka)^{1/\nu}, h/(ka)^{\beta\delta/\nu}\right), \tag{5.13}$$

where, using (5.2),

$$Z(u,v) = \hat{G}(a^{-1},u,v)/\hat{G}(a^{-1},0,0)\,, \tag{5.14}$$

so that $Z(0,0)=1$. Although this represents the critical point limit simply, it does not describe the low-momentum, $k\to 0$ $(h,t\neq 0)$, limit transparently. Since data on the low momentum limit are more readily available and more accurate, both experimentally (from low angle scattering) and theoretically (from series expansions), this is a fairly serious inconvenience. Accordingly, we now develop a form which is theoretically more elaborate but which seems more practical for the representation of the series data and for analyzing experimental observations.

By taking the $k\to 0$ limit in (5.1) we can write

$$\hat{\Gamma}(\vec{k},H,T) \approx \chi_0(H,T)\frac{\hat{G}(k\lambda, t\lambda^{1/\nu}, h\lambda^{\beta\delta/\nu})}{\hat{G}(0, t\lambda^{1/\nu}, h\lambda^{\beta\delta/\nu})}\,, \tag{5.15}$$

where χ_0 is given in scaling form by (4.3), or in parametric form by (4.6)–(4.8). Now we choose $\lambda=\xi_1$ where $\xi_1(H,T)$ is given in terms of a scaling function $Y(z)$ in (5.3), and parametrically via (5.4). This leads to our final form

$$\hat{\Gamma}(\vec{k},H,T) \approx \chi_0(H,T)\hat{D}(k^2\xi_1^2, h/|t|^{\beta\delta})\,, \tag{5.16}$$

where, with $\sigma=-1/2\nu$ and $\tau=-\beta\delta/2\nu$, one has

$$\hat{D}(x^2,z) = \frac{\hat{G}(x, \pm[y_0Y(z)/a]^{\sigma}, z[y_0Y(z)/a]^{\tau})}{\hat{G}(0, \pm[y_0Y(z)/a]^{\sigma}, z[y_0Y(z)/a]^{\tau})}\,. \tag{5.17}$$

The $\pm$ signs refer to $t\geq 0$ or $t\leq 0$, respectively, and the appropriate form of $Y(z)$ must be similarly used. Thus, $\hat{D}(x^2,z)$ consists of two parts matching as $z\to\infty$; for brevity, however, we will not normally indicate this explicitly. The various exponent relations quoted in Sec. II E follow from (5.16) in the standard way[2,8] subject only to the nonvanishing of various limiting amplitudes.[2c]

On the three principal loci; critical isochore, critical isotherm, and phase boundary $\hat{D}(x^2,z)$ reduces to three single-variable scaling functions[9]

$$\begin{aligned} &\hat{D}(x^2,0)_{t>0} = \hat{D}^+(x^2),\quad \hat{D}(x^2,\infty) = \hat{D}^c(x^2)\,,\\ &\hat{D}(x^2,0)_{t<0} = \hat{D}^-(x^2)\,. \end{aligned} \tag{5.18}$$

The function $\hat{D}^+(x^2)$ was studied intensively in Parts I and II.

By considering small $k\xi_1$ in (5.16) we see that the scaling function must satisfy the normalization relations

$$\hat{D}(0,z)=1 \quad \text{all } z\,, \tag{5.19}$$

$$(d\hat{D}/dx^2)_{x=0} = -1 \quad \text{all } z\,. \tag{5.20}$$

Evidently we may regard $\hat{D}(x^2,z)$ as a normalized *scattering line-shape function.*

In order to reproduce the correct critical point behavior (2.16) [or satisfy (5.2)] the scaling function for $x\to\infty$ must vary as

$$\hat{D}(x^2,z) \approx \tilde{D}_\infty(z)/x^{2-\eta}\,, \tag{5.21}$$

where

$$\tilde{D}_\infty(z) = Q_3/X(z)[Y(z)]^{1-\eta/2}\,, \tag{5.22}$$

in which the dimensionless parameter Q_3 is defined by

$$Q_3 = \hat{D}(f_1^+)^{2-\eta}/C^+ = \tilde{D}_\infty(0) = \tilde{D}_\infty^+\,. \tag{5.23}$$

The data of Parts I and II (see Table I) support reasonably well the expectation that Q_3 should have a universal value. We adopt the value $Q_3 = 0.899 \pm 0.006$.

These results may be written somewhat more simply in terms of the parametric representation. Thus by (4.6) we may substitute for the variable z in favor of θ since one has

$$z = h/t^{\beta\delta} = z(\theta) = l(\theta)/[k(\theta)]^{\beta\delta}\,. \tag{5.24}$$

Then using (4.8), (4.11), and (5.4), one can write

(5.22) as

$$\tilde{D}_\infty(\theta) = Q_3/\tilde{p}(\theta)[\tilde{y}(\theta)]^{1-\eta/2}. \tag{5.25}$$

For small values of x (i.e., $k \to 0$) we expect[2,4] an expansion of the form

$$1/\hat{D}(x^2, z) = 1 + x^2 - \Sigma_4(z)x^4 + \Sigma_6(z)x^6 + \cdots. \tag{5.26}$$

The first two terms follow from (5.19) and (5.20). The coefficient $\Sigma_4(z)$ measures the first deviation from the Lorentzian line shape of the scattering away from the critical point. We will present estimates for Σ_4 on the principal loci. (For $T > T_c$ estimates are implicit in Parts I and II.) Values of Σ_4 and Σ_6 have been calculated by renormalization group techniques[22] to order ϵ^2. All the coefficients Σ_{2k} ($k \geq 2$) vanish identically in mean-field theory, and in the Elliott-Marshall-Bethe (EMB), and Ornstein-Zernike approximations, so that $\hat{D}(x^2, z) = (1 + x^2)^{-1}$, independently of z. This simple result provides an indication of the usefulness of the representation (5.16).

The asymptotic form (5.21) for large x may similarly be extended. One expects[2,4,23,24]

$$\hat{D}(x^2, z) \approx \tilde{D}_\infty(z)/x^{2-\eta} + \tilde{D}_{\infty,1}(z)/x^{2-\eta+(1-\alpha)/\nu} + \tilde{D}_{\infty,2}(z)/x^{2-\eta+1/\nu} + \cdots \tag{5.27}$$

as $x \to \infty$, where α is the specific-heat exponent. The form of the correction terms in this expansion is of considerable interest[23] and has recently been the subject of an $\epsilon = 4 - d$ expansion calculation[22] which confirmed (5.27) and gave explicit expressions for $\tilde{D}^+_\infty$, $\tilde{D}^+_{\infty,1}$, and $\tilde{D}^+_{\infty,2}$ (i.e., for $H = 0$, $T > T_c$) correct to order ϵ^2. The leading correction introduces a term which mirrors the energy, $\sim t^{1-\alpha}$, in the variation of $\hat{\Gamma}(\vec{k}, T, 0)$ at fixed k as $T \to T_c+$. This behavior has been detected in observations of the critical resistivity of ferromagnets[23b] but is very hard to see directly in scattering experiments. The correction amplitudes $\tilde{D}_{\infty,1}$ and $\tilde{D}_{\infty,2}$ are also difficult to estimate reliably by series expansion techniques but in Sec. VIID we discuss the estimation of the leading correction in (5.27) and quote a numerical estimate for $\tilde{D}^-_{\infty,1}$. [It may be mentioned that a more recent renormalization group analysis[25] indicates the nature of the higher-order terms in (5.27).]

C. Scaling function approximants

The mean-field scaling function, $\hat{D}(x^2, z) = (1 + x^2)^{-1}$ cannot satisfy (5.21) for nonzero η. The simplest function which will accomodate a nonvanishing value of η is the "zeroth-order approximant" of Part I, namely,

$$\hat{D}_0(x^2, z) = 1/(1 + \psi x^2)^{1-\eta/2}, \tag{5.28}$$

with $\psi = (1 - \frac{1}{2}\eta)^{-1}$ in order to preserve the normalization (5.20). Although as shown in Part I, this is a tolerable, rough approximation on the critical isochore ($H = 0$, $T > T_c$) for $d = 3$, it fails more seriously in nonzero field and below T_c; in particular, the predicted value of $\tilde{D}_\infty(z)$ is not accurate even for $z = \theta = 0$, and it will be worse elsewhere.

In order to be able to match the correct value of $\tilde{D}_\infty(0) = Q_3$ above T_c, Fisher and Burford (FB)[4] introduced the approximant

$$\hat{D}_{\mathrm{FB}}(x^2) = \frac{(1 + \phi^2 x^2)^{\eta/2}}{1 + \psi x^2}, \tag{5.29}$$

with parameters chosen according to

$$\psi = 1 + \tfrac{1}{2}\eta\phi^2 \tag{5.30}$$

and

$$\phi^\eta/(1 + \tfrac{1}{2}\eta\phi^2) = \tilde{D}_\infty(0) = Q_3. \tag{5.31}$$

(The first condition is again required to satisfy the normalization.) In Part I this was shown to be a very satisfactory approximant: in particular if k^2 was replaced by the effective wave number $K^2(\vec{k})$ defined in (3.2), and if ϕ was allowed to become temperature dependent outside the critical region, the approximant worked well for *all* $\vec{k}$ and T. [In this case, ϕ, in (5.31) is to be replaced by $\phi_c = \phi(T_c)$.] An especially significant feature of the approximant $\hat{D}_{\mathrm{FB}}(x^2)$ is that the nearest singularity (assuming $\psi > \phi^2$), is a pair of simple poles on the imaginary x axis at $x_0 = \pm i\psi^{-1/2}$. As discussed in I (and Refs. 2 and 26) this corresponds to the Ornstein-Zernike decay law $\Gamma(\vec{R}) \sim e^{-\kappa R}/R^{(d-1)/2}$, with

$$\kappa = |x_0|/\xi_1, \tag{5.32}$$

and is expected to be a characteristic of the exact scaling function. Indeed this should still be true[2,26] for nonzero fields, and also below T_c in zero field (except for the two-dimensional, nearest-neighbor Ising model; see below[26]). Unfortunately, if the Fisher-Burford approximant form is tried for general z or θ, the corresponding equation for $\phi(z)$, namely, (5.31) with Q_3 replaced by $\tilde{D}_\infty(z)$ from (5.22) or (5.25), is found to have no real root on the critical isotherm or below T_c. [This is simply because the maximum value of $\phi^\eta/(1 + \frac{1}{2}\eta\phi^2)$ is $(1 - \frac{1}{2}\eta)^{(2-\eta)/2} < 1$, while it follows from the data of Table I that the required values rise to 1.26 and 2.26 times this value below T_c for $d = 3$ and 2, respectively.]

In order to solve this problem one may adopt a purely *ad hoc* approach. Thus the form

$$\hat{D}_A(x^2) = \frac{(1 + \phi'^2 x^2)^{\sigma+\eta/2}}{(1 + \psi' x^2)(1 + \phi''^2 x^2)^\sigma} \tag{5.33}$$

with, for normalization,

$$\psi' = 1 + \tfrac{1}{2}\eta\phi'^2 + \sigma(\phi'^2 - \phi''^2) \tag{5.34}$$

and

$$\phi'^{2\sigma+\eta}/\psi'\phi''^{2\sigma} = \tilde{D}_\infty, \tag{5.35}$$

is more flexible and, we will show[9] in Sec. VIII, can provide acceptable fits to the data at and below T_c. As in $\hat{D}_{\text{FB}}(x^2)$, the nearest singularity is a simple pole (provided ϕ'^2 and ϕ''^2 are less than ψ, as in fact transpires). A drawback is that the number of free parameters is more than required at first sight. However, one of the parameters can be chosen so as to obtain the correct value of Σ_4. (The higher order Σ_{2k} are too uncertain numerically to be useful.) The exponent σ should be small for reasons to be indicated shortly. (Values around η or 2η are found to work, as shown in Sec. VIII, but the residual arbitrariness is unsatisfying.) A second drawback of this form is that it cannot go smoothly over into the FB form as $\theta \to 0$ (i.e., as $H \to 0$ above T_c) unless the exponent σ is allowed to vary with θ, which seems very artificial: It would be desirable merely to have coefficients, like ϕ' and ϕ'', vary. We also expect these coefficients to be not extraordinarily small (since otherwise the approximant will vary with unreasonable rapidity at large x).

A more systematic approach to generalizing the FB approximant is to inquire more closely into the probable singularity structure of the correlation function, assuming that this, in turn, will be reflected in the scaling functions. As discussed in I, and more generally in Refs. 26, one expects that the "single particle" poles in $\hat{\Gamma}(\vec{k})$ at $k = \pm i\kappa$ are accompanied by "multiparticle" branch cuts located at $\pm 2i\kappa$, $\pm 3i\kappa, \ldots$. However, for reasons of symmetry the "even-particle" singularities at $\pm 2i\kappa$, $\pm 4i\kappa, \ldots$ will be absent in zero field above T_c. The absence of the two-particle cut seems to be the basic reason why the FB approximant works so well on the critical isochore. The numerator factor $(1+\phi^2 x^2)^{\eta/2}$ in $D_{\text{FB}}(x^2)$ introduces a weak branch point at $x = \pm i\phi^{-1}$ (which turns out numerically to correspond to about[4,5] $\pm 7i\kappa$ for $d=3$ and $\pm 34i\kappa$ for $d=2$) and thus represents the average effects of the higher, odd branch points.

The nature of the next-nearest, or two-particle branch point has been discussed by Fisher and Camp[26] who conclude that in real space it corresponds to an additive contribution to $\Gamma(\vec{R})$ decaying as

$$e^{-2\kappa R}/R^d, \text{ as } R \to \infty, \tag{5.36}$$

compared with the dominant single-particle pole, which leads to the Ornstein-Zernike decay $e^{-\kappa R}/R^{(d-1)/2}$, as already mentioned. Fourier transformation then leads to the conclusion that the scaling function should have singularities of the form

$$d=2: \ (4|x_0|^2 + x^2)^{1/2}, \tag{5.37}$$

$$d=3: \ (4|x_0|^2 + x^2)\ln(4|x_0|^2 + x^2), \tag{5.38}$$

as $x \to \pm 2i|x_0|$ assuming there are poles at $\pm i|x_0|$. At the higher-order branch cuts the singularities will be correspondingly weaker. [This is why one expects a small exponent σ in the *ad hoc* approximant (5.33)]; similarly one expects $\phi'^2, \phi''^2 \lesssim \frac{1}{4}\psi$ to ensure no singularities closer than the two-particle branch points.

These considerations suggest as a possible approximant for *three dimensions*, the form

$$\hat{D}_B(x^2, z) = \frac{(1+\phi^2x^2)^{\eta/2}}{1+\psi x^2} \times \left[1 - \lambda + \lambda\frac{(1+\frac{1}{4}\psi x^2)}{2\ln\omega}\ln\left(\frac{\omega^2 + \frac{1}{4}\psi x^2}{1+\frac{1}{4}\psi x^2}\right)\right]. \tag{5.39}$$

The first factor here is just the FB approximant, to which $\hat{D}_B(x^2, z)$ reduces if one chooses $\lambda(z) \to 0$ as z, $\theta \to 0$. The modification factor introduces the desired logarithmic branch points at $\pm 2i|x_0|$, where the poles occur at $\pm i|x_0| = \pm i\psi^{-1/2}$. As before, the parameter ψ is chosen to preserve the normalization which yields

$$\psi = (1+\tfrac{1}{2}\eta\phi^2)/\{1 - \tfrac{1}{4}\lambda[1-(\omega^2-1)/2\omega^2\ln\omega]\}. \tag{5.40}$$

Similarly, as a function of z or θ, one must satisfy

$$\phi^\eta[1 - \lambda + \tfrac{1}{2}\lambda(\omega^2-1)/\ln\omega] = \psi\tilde{D}_\infty(z). \tag{5.41}$$

If the parameter ϕ is held fixed at its value on the critical isochore ($z = \theta = 0$) this represents a relation between $\lambda(z)$ and $\omega(z)$. The parameter ω should exceed $\frac{3}{2}$ to ensure that there are no other singularities closer than the three-particle branch points at $\pm 3i|x_0|$ (which are not, of course, properly represented by the approximant). Subject to this, another relation may be obtained by matching $\Sigma_4(z)$. Of course, we could also choose to vary ϕ with z or θ.

It should be stressed that none of the scaling function approximants discussed so far reproduce correction terms to the large-x behavior of the form expected according to (5.27), i.e., they will all fail to reproduce an energy or $t^{1-\alpha}$-type singularity at fixed momentum k as $T \to T_c$.[23-25] Above T_c this defect is probably not very serious numerically in most situations. Below T_c (and, to a somewhat lesser extent, at T_c) one must expect the inaccuracies to be more significant, basically because the deviations from the Ornstein-Zernike form turn out to be much larger. However, it is difficult to devise simple approximants of the desired form and, as mentioned, not easy to estimate the required amplitudes numerically (although some progress is reported in Sec. VII D, below). Accordingly, no serious efforts have been made to remedy the defect.

We will discuss the application of the three-dimensional approximant (5.39) in further detail in Sec. VIII.

The behavior of the *two-dimensional* correlation function below T_c in zero field is very special[26] in that the dominant decay is known exactly[27-29] to be of the form $e^{-\kappa R}/R^2$. This corresponds to a branch singularity of the form (5.37) rather than to the simple poles that might have been expected.[26] The absence of the simple poles means that none of the approximants discussed above can be considered reasonable below T_c. One of the simplest possibilities with the correct nearest singularity for *two dimensions* is[9]

$$\hat{D}_C(x^2) = 1/[1 - \lambda + \lambda(1 + \psi' x^2)^{1/2}]^{2-\eta}. \tag{5.42}$$

If ψ' and λ are chosen, as before, to match the small-x and large-x conditions, one obtains a prediction for the position of the branch points, at $x = \pm i \psi'^{-1/2}$. As before, this yields an estimate of the true, exponential range of correlation. However, this information is known exactly from the analytical solutions of the square Ising lattice.[27-29] In particular one finds[27-29]

$$f^+/f^- = 2\,, \tag{5.43}$$

for the true ranges (which may be compared with the estimate $f_1^+/f_1^- \simeq 3.23$ obtained below, and already quoted in Table I). Knowledge of f^- together with an estimate of f_1^- shows that the branch points should be located at

$$x = \pm i(f_1^-/f^-)\,. \tag{5.44}$$

As a matter of fact, using the approximant (5.42) leads to surprizingly good consistency with (5.43). However, better accuracy can be obtained by the slightly more elaborate *two-dimensional* approximant

$$\hat{D}_D^-(x^2) = \frac{(1 + \phi'^2 x^2)^{\eta/2}}{[1 - \lambda + \lambda(1 + \psi' x^2)^{1/2}]^2}\,, \tag{5.45}$$

where, now, the correct location of the branch point is ensured by the choice

$$\psi' = (f^-/f_1^-)^2\,. \tag{5.46}$$

In addition, the normalization conditions yield

$$\lambda = (1 + \tfrac{1}{2}\eta\phi'^2)/\psi' \tag{5.47}$$

and

$$\phi'^{\eta}/\lambda^2\psi' = \tilde{D}_\infty^-\,. \tag{5.48}$$

Further parameters could be introduced, in principle, to match Σ_4^- but since, as it turns out, Σ_4 cannot be estimated numerically with much precision, this does not seem worthwhile. Again, it must be noted that these two-dimensional scattering approximants will *not* reproduce the expected energylike singularity (in this case $\sim t\ln|t|$) in the scattering at fixed $\vec{k}$ as $T \to T_c$. This will be an inevitable source of inaccuracy at large x.

Various possibilities suggest themselves when it comes to attempting to generalize (5.45) to nonzero fields so as, hopefully, to transform smoothly to the FB form as z or $\theta \to 0$. In this region above T_c, when $d=2$, we expect the square root branch point contained in (5.45) to correspond to two-particle singularities at $\pm 2i|x_0|$ (with the poles at $\pm i|x_0|$). However, it is *not* clear what the relation between pole and branch point should be below T_c in small fields. For this reason, and because of additional numerical fitting difficulties encountered, with various trial forms, we will not discuss the problem of field-dependent approximants further here. We mention, however, that the *ad hoc* approximant $\hat{D}_A(x^2)$ of (5.33) may be used *on* the critical isotherm for $d=2$ (where a pole is expected to dominate). The detailed application of the two-dimensional approximants is again postponed to Sec. VIII.

VI. CALCULATION OF SERIES EXPANSIONS

A. General considerations

The aim of the calculations described in this section is to obtain the series expansion for the correlation function $\Gamma(\vec{R}, H, T)$ in powers of the temperature and field variables u (or x) and y defined in (2.2). The expansion may be written

$$\Gamma(\vec{R}, H, T) = y u^{q/2} \sum_{k=0}^{\infty} \sum_{l=0}^{\bar{l}(k)} q_{kl}(\vec{R}) u^{qk/2 - l} y^k\,, \tag{6.1}$$

where q is again the lattice coordination number. The upper limit $\bar{l}(k)$ is equal to the maximum number of (internal) bonds that can be formed in a cluster of $k+1$ sites on the lattice; it is less than or equal to $\frac{1}{2}qk$ so that the lowest power of u in the sum is always non-negative; furthermore, this lowest power generally increases with k. By setting u equal to its critical value, $u_c = \exp(-4J/k_B T_c)$, series in the single variable y are obtained for the critical isotherm; by setting $y=1$ (or $H=0+$) a low-temperature series in powers of u is found for the phase boundary. Readers uninterested in the details of the calculation of the coefficients $q_{kl}(\vec{R})$ may omit this whole section.

Through the Fourier relation (2.8), which is readily programmed for handling power-series representations, it is sufficient to know the corresponding expansion for the inverse correlation function,

$$\mathcal{C}(\vec{R}) = y^{-1}u^{-q/2}\sum_{k=0}^{\infty}\sum_{l=0}^{\bar{l}(k)} c_{kl}(\vec{R})u^{qk/2-l}y^k . \qquad (6.2)$$

Accordingly our basic results are presented for the inverse correlation function (see Appendix A).

As sketched in Sec. VI B below, the series (6.1) may be constructed directly by the method of enumeration of spins "overturned" from a fully ordered configuration.[30] This method is most effective for calculating the series in powers of u alone, to a given order; it has been used in the present work to obtain extra terms q_{kl} for large l (corresponding to compact clusters of relatively many spins). On the other hand, the general term in y^k, representing essentially k overturned spins, involves many separated and noncompact configurations which are hard to count correctly. We have found the semi-invariant expansion for the Ising model[31-33] more effective in this case; the method employed is outlined in Sec. VI C below. This approach leads to the "high-temperature" expansion

$$\mathcal{C}(\vec{R}, H, T) = y^{-1}\sum_{k=0}^{\infty}\sum_{l=0}^{\infty}\tilde{c}_{kl}(\vec{R})K^l y^k , \qquad (6.3)$$

in powers of $K = J/k_BT$. However, by expanding $u = e^{-4K}$ in powers of K in (6.2) (for fixed y) and comparing coefficients with (6.3) one obtains sets of $[\bar{l}(k)+1]\times[\bar{l}(k)+1]$ linear equations for the coefficients $c_{kl}(\vec{R})$ in terms of the $\tilde{c}_{kl}(\vec{R})$. These are readily inverted by machine to yield the desired expansion (6.2).

B. Low-temperature high-field expansion

As explained by Domb,[30] the low-temperature high-field expansion starts with a fully magnetized configuration in which all N spins point "up." If now N_1 spins are turned "down" to form a configuration with N_{12} unlike pairs of spins or "wrong" bonds, the energy of the configuration for nearest-neighbor interactions with coordination number q, is simply

$$E(N_1, N_{12}) = -\tfrac{1}{2}qNJ - NmH + 2N_{12}J + 2N_1 mH . \quad (6.4)$$

The partition function can thus be written

$$Z_N(H, T) = u^{-Nq/8}y^{N/2} \times \sum_{N_1, N_{12}} g_N(N_1, N_{12})u^{N_{12}/2}y^{N_1}, \qquad (6.5)$$

where $g_N(N_1, N_{12})$ is the number of distinct configurations of N_1 overturned spins forming N_{12} wrong bonds on the lattice of N spins. It is appropriate to take a large lattice with periodic boundary conditions. In that case $g_N(N_1, N_{12})$ for $N \gg N_1, N_{12}$, is simply a polynomial in N. The expansion for the limiting free energy

$$F(H, T)/k_BT = \lim_{N\to\infty} N^{-1}\ln Z_n(H, T) , \qquad (6.6)$$

is then obtained formally from (6.5) by retaining only the coefficient, $g_{(1)}(N_1, N_{12})$, of N^1 in the polynomial $g_N(N_1, N_{12})$.

The spin-pair correlation function $\langle s_{\vec{0}}s_{\vec{R}}\rangle$ can be obtained by a similar construction in which, however, the configurations of the spins at $\vec{0}$ and $\vec{R}$ are held fixed "up" (or +) or "down" (or −). If the number of these configurations is $g_N^{++}(N_1, N_{12}, \vec{R})$, etc., we have

$$\langle s_{\vec{0}}s_{\vec{R}}\rangle = u^{-Nq/8}y^{N/2}[Z_N(H, T)]^{-1} \times \sum_{N_1, N_{12}} g_N^2(N_1, N_{12}, \vec{R})u^{N_{12}/2}y^{N_1} ,$$

with (6.7)

$$g_N^2(N_1, N_2, \vec{R}) = g_N^{++}(N_1, N_{12}, \vec{R}) - 2g_N^{+-}(N_1, N_{12}, \vec{R}) + g_N^{--}(N_1, N_{12}\vec{R}) .$$

It then follows that the coefficient of $u^{N_{12}/2}y^{N_1}$ in the expansion of $\langle s_{\vec{0}}s_{\vec{R}}\rangle$ may be found formally as the coefficient, $g_{(0)}^2(N_1, N_{12}, \vec{R})$, of N^0 in the expression for $g_N^2(N_1, N_{12}, \vec{R})$, which, for sufficiently large N, is also a polynomial in N.

C. Semi-invariant expansion for the Ising model

The semi-invariant approach for the Ising model yields an expansion in powers of K for general field $H = Lk_BT/m$. We outline the discussion of Englert[33] and indicate later refinements developed by Jasnow and Wortis,[34] and Wilson.[35]

Consider the thermal expectation of a product of a set P of p spins at sites $\vec{R}_\pi (\pi \in P)$, namely,

$$\langle s_P\rangle = \left\langle \prod_{\pi\in P} s_{\vec{R}_\pi}\right\rangle . \qquad (6.8)$$

This may be written

$$\langle s_P\rangle = \frac{\left\langle s_P \exp\left(K\sum_{(\vec{R},\vec{R}')} s_{\vec{R}}s_{\vec{R}'}\right)\right\rangle_0}{\left\langle \exp\left(K\sum_{(\vec{R},\vec{R}')} s_{\vec{R}}s_{\vec{R}'}\right)\right\rangle_0} , \qquad (6.9)$$

where the summation runs over all distinct nearest-neighbor bonds $(\vec{R}, \vec{R}')$, while the subscript 0 denotes an expectation taken in the uncoupled Hamiltonian with $K = 0$. Expansion of the exponential in powers of K then yields a graphical expansion for $\langle s_P\rangle$ as a sum over p-rooted, weighted graphs; that is,

$$\langle s_P\rangle = \sum_{G^{(p)}} W(G^{(p)})\,. \qquad (6.10)$$

The rules for the graphs[36] and the weights W are the following:

(a) The sum runs over all undirected, labeled, linked graphs $G^{(p)}$ with p root points. (Multibonds are allowed and regarded just as a collection of distinct simple bonds or lines.)

(b) Each vertex i of a graph $G^{(p)}$ is associated with a lattice site $\vec{R}_i$, each root point (or external vertex[36] $i\equiv\pi=1,2,\ldots p$ being associated with the corresponding (fixed) spin site $\vec{R}_\pi$ $(\pi\in P)$.

(c) Each *internal* vertex (non root point) i of degree n (i.e., at which n bonds meet, counting each component of any multibond) is given a vertex weight $w_i = M_n^0(L)$ where, for the spin-$\frac{1}{2}$ Ising model, the bare semi-invariants $M_k^0(L)$ may be defined by

$$M_k^0(L) = (d/dL)^k M_0^0(L)\,,\quad M_0^0(L) = \ln(2\cosh L)\,. \qquad (6.11)$$

(d) Each root point, i, of $G^{(p)}$ of degree n is assigned a vertex weight $w_i = M_{n+1}^0(L)$.

(e) Each line or bond, (i,j), of $G^{(p)}$ is assigned a bond weight w_{ij} which, for nearest-neighbor interactions is equal to $K\Delta(\vec{R}_j-\vec{R}_i)$, where

$$\begin{aligned}\Delta(\vec{R}) &= 1 \text{ if } |\vec{R}| = a\,,\\ &= 0 \text{ if } |\vec{R}| \neq a\,,\end{aligned} \qquad (6.12)$$

(so that Δ vanishes unless $\vec{R}$ is a nearest-neighbor vector $\vec{\delta}$).

(f) The total weight of a graph $G^{(p)}$ is defined by

$$W(G^{(p)}; \vec{R}_1,\ldots \vec{R})_p = [s(G^{(p)})]^{-1} \times \sum_{\vec{R}_i} \prod_i w_i \prod_{(ij)} w_{ij}(\vec{R}_i,\vec{R}_j)\,, \qquad (6.13)$$

where the summations run only over the coordinates $\vec{R}_i$ of the internal points of $G^{(p)}$ (the root-point coordinates being held fixed), while $s(G^{(p)})$ is the symmetry number[36] of $G^{(p)}$.

For a given lattice $\mathfrak{L}$, the expression for the total weight can be simplified for a graph of $l(G^{(p)})$ bonds to

$$W(G^{(p)};\vec{R}_1,\ldots\vec{R}_p) = \langle G^{(p)},\mathfrak{L};\vec{R}_1,\ldots\vec{R}_p\rangle K^{l(G^{(p)})}\prod_i w_i\,, \qquad (6.14)$$

where the "embedding constant" is defined by

$$\langle G^{(p)},\mathfrak{L};\vec{R}_1,\ldots\vec{R}_p\rangle = \sum_{\vec{R}_i}\prod_{(ij)}\Delta(\vec{R}_j-\vec{R}_i)\,. \qquad (6.15)$$

As before the product runs over all bonds of $G^{(p)}$ and the sum over the coordinates of all internal vertices. Evidently the embedding constant for the two-rooted single bond $K_2^{(2)}$ is simply $\langle K_2^{(2)},\mathfrak{L};\vec{R}_1,\vec{R}_2\rangle = \Delta(\vec{R}_2-\vec{R}_1)$, for all $\mathfrak{L}$. (In the terminology of Ref. 36 this embedding constant may be regarded as a "free lattice constant" since, in contrast to the definition of "weak lattice constants," distinct vertices of $G^{(p)}$ need not be embedded in distinct vertices of $\mathfrak{L}$.)

The calculation of the embedding constants needed for evaluating $\langle s_{\vec{0}} s_{\vec{R}}\rangle$ in zero field (above T_c) has been considered in detail by Jasnow.[34] However, since the odd semi-invariants vanish when $L=H=0$, only graphs with internal vertices of even degree and external vertices of odd degree are then required. For the present work graphs with all vertex degrees must be included. The calculations are simplified, however, by noting that the skeleton graph $G^{(p)\times}$, derived from $G^{(p)}$ by replacing all multibonds by simple bonds, has the same lattice constant as $G^{(p)}$. Furthermore, if $G^{(p)}$ is the union of disjoint connected components $G_1^{(p_1)}, G_2^{(p_2)},\ldots,$ the embedding constant for $G^{(p)}$ is just the product of the separate embedding constants for the connected components. We have thus needed to consider a total of 124 two-rooted and one-rooted connected skeleton graphs.

Further economy results from a simple lemma which follows directly from the definition (6.11), namely: if $G^{(p)} = G_1^{(2)}\cup G_2^{(2)}\cup\ldots\cup G_\alpha^{(2)}\cup\ldots$ can be dissected into a set of connected two-rooted graphs $G_\alpha^{(2)}$ with disjoint sets of internal vertices, then

$$\langle G^{(p)},\mathfrak{L};\vec{R}_1,\ldots\vec{R}_p\rangle = \sum_{\vec{R}_k}\prod_\alpha\langle G_\alpha^{(2)},\mathfrak{L};\vec{R}_{\alpha 1},\vec{R}_{\alpha 2}\rangle\,, \qquad (6.16)$$

where there the sum runs over the coordinates $\vec{R}_k = \vec{R}_{\alpha i}\equiv\vec{R}_{\alpha' i'},\ldots,$ of each root point which is not also a root point of $G^{(p)}$. In an extreme case the components $G_\alpha^{(2)}$ will just be simple bonds $K_2^{(2)}$ and then (6.16) reduces to (6.15). More generally they will be two-pieces[36] of $G^{(p)}$.

The number of graphs needed can be greatly reduced by introducing renormalized semi-invariants $M_n(K,L)$. To define these we first introduce a series of functions $E_m(K;M_0,M_1,\ldots)$, the renormalized self-energies, defined graphically by

$$E_m(K;M_0,M_1,\ldots) = \sum_{G^{(1)}} W(G^{(1)})\,, \qquad (6.17)$$

where (a) the sum now runs only over those singly rooted linked graphs in which the root point has degree m, and which contain no articulation points,[36] and

(b) the graph weights are given by (6.13) or (6.14) except that the vertex weight of an internal vertex of degree n is now M_n (in place of M_n^0) while the root point is assigned weight unity. (We have departed from the customary notation where the nth-order renormalized self-energy is denoted by G_n.) The renormalized semi-invariants are now defined implicitly by

$$M_n(K, L) = \left\{ \exp\left[\sum_{m=0}^{\infty} E_m(K; M_1, M_2, \ldots)\left(\frac{d}{dL'}\right)^m \right] \times M_n^0(L') \right\}_{L'=L} . \quad (6.18)$$

If the graphs are ordered according to their number of bonds and one recalls (6.11), it is not hard to see that these equations may be solved recursively to yield the renormalized semi-invariants as power series in K with coefficients which are polynomials in the bare semi-invariants $M_n^0(L)$. In practice we compute the bare semi-invariants as power series in y. The descriptions of all the self-energy graphs of l lines, including their symmetry number, and the degrees of each vertex are then read into a program which performs the inversion and computes the renormalized semi-invariants as power series in y and K.

The renormalized semi-invariants could now be used to compute the averages $\langle s_p \rangle$ by modifying the definition of the vertex weights and restricting the summation in (6.10) to linked graphs with no articulation points.[36] In particular, in the sum for $\Gamma(\vec{R})$ disconnected graphs cancel between $\langle s_{\vec{0}} s_{\vec{R}} \rangle$ and $\langle s_{\vec{0}} \rangle \langle s_{\vec{R}} \rangle$. Thus one requires only the single vertex, which contributes $M_2 \delta_{\vec{0}\vec{R}}$, and those two-rooted graphs whose derived graphs are stars.[36]

However, the number of graphs needed to compute $\Gamma(\vec{R})$ can be reduced considerably by defining the function $\Phi(\vec{R})$ to be the sum of only those contributions to $\Gamma(\vec{R})$ where the associated graph $G^{(2)}$ has no cut edge[36] (removal of which would decompose $G^{(2)}$ into two disconnected components still, however, linked through the roots). Note that $\Phi(\vec{R})$ includes a contribution from the single vertex. A little consideration shows that $\Phi(\vec{R})$ must satisfy the equation[34,35]

$$\Gamma(\vec{R}) = \Phi(\vec{R}) + K \sum_{\vec{R}', \vec{R}''} \Gamma(\vec{R}'')\, \Delta(\vec{R}'' - \vec{R}')\Phi(\vec{R}' - \vec{R}) . \quad (6.19)$$

On taking Fourier transforms this becomes

$$\hat{\mathcal{C}}(\vec{k}) = 1/\hat{\Gamma}(\vec{k}) = [\hat{\Phi}(\vec{k})]^{-1} - K \sum_{\vec{\delta}} e^{i\vec{k}\cdot\vec{\delta}} , \quad (6.20)$$

which may be inverted finally to yield

$$\mathcal{C}(\vec{R}) = \tilde{\Phi}(\vec{R}) - K\Delta(\vec{R}) , \quad (6.21)$$

where

$$\tilde{\Phi}(\vec{R}) = \int d\vec{k}\, e^{i\vec{k}\cdot\vec{R}}/\hat{\Phi}(\vec{k}) , \quad (6.22)$$

in which the wave-vector integral runs over the appropriate Brillouin zone. Thus, knowledge of $\Phi(\vec{R}, K, L)$ is sufficient to yield the inverse correlation function $\mathcal{C}(\vec{R}, H, T)$, and $\Phi(\vec{R})$ may be generated as a sum of connected, two-rooted graphs with no articulation points and no cut edges.

We have utilized an enumeration[35] of all graphs of up to nine lines needed for the self-energies E_m and the function $\Phi(\vec{R})$ on loose-packed lattices (i.e., with no triangular subgraphs); there are 287 singly rooted graphs, contributing to E_m, and 954 doubly rooted graphs contributing to $\Phi(\vec{R})$, corresponding to the 124 skeleton graphs mentioned above. This then yields the expansion (6.3) to order K^9 which is sufficient to obtain the coefficients c_{kl} in (6.2) complete for $k \leq 7$ for the sc and square lattices and for $k \leq 6$ for the bcc lattice.[37] This corresponds to all configurations of 8 and 7 overturned spins, respectively. The series in u for $y = 1$ were extended, as mentioned, by using the direct enumeration method. In this way, 13 terms in powers of u were obtained for the sc lattice, 16 for the bcc, but only six for the square lattice.[37] The results are tabulated in Appendix A.

Once the series have been generated there are several checks available. The expansion for the susceptibility can be calculated from

$$\chi_0 = 1/\hat{\mathcal{C}}(\vec{0}) = \hat{\Gamma}(\vec{0}) \quad (6.23)$$

and the energy per spin, U, is given by

$$U = -\tfrac{1}{2} qJ[\Gamma(\vec{\delta}) + \langle s_{\vec{0}} \rangle^2] . \quad (6.24)$$

Series for these quantities are available[38a] and have provided an important check of our results.

VII. SERIES ANALYSIS

A. Critical points and exponents

In this section we analyze series for moments of the correlation function, etc., below T_c in zero field, i.e., along the phase boundary, and *at* T_c as a function of field, i.e., on the critical isotherm. We test the scaling predictions for the exponents ν' and ν^c, and, assuming the scaling values for these exponents, we estimate various critical amplitudes. In addition we discuss the true range of correlation below T_c, and test strong scaling and the spherical symmetry of the correlation function as $T \to T_c -$.

In all the analyses we use the exact value

$$u_c = 3 - 2\sqrt{2} = 0.1715728\ldots, \tag{7.1}$$

for the critical point of the square lattice,[2b] and the estimates

$$u_c = 0.411985 \pm 14 \quad (\text{sc}), \tag{7.2}$$

$$u_c = 0.532789 \pm 26 \quad (\text{bcc}), \tag{7.3}$$

found by Sykes *et al.*[38bc] for the sc and bcc lattices. The uncertainties in these values (quoted in units of the last decimal place) will not affect any of our numerical work to within the precision available. As regards the exponents, all the values

$$\beta = \tfrac{1}{8}, \quad \gamma = \gamma' = 1\tfrac{3}{4}, \quad \delta = 15,$$

$$\nu = \nu' = 1, \quad \eta = \tfrac{1}{4}, \quad (d=2), \tag{7.4}$$

may be regarded as exact for the two-dimensional Ising model.[2b] For the three-dimensional lattices we will adopt

$$\beta = \tfrac{5}{16}, \quad \gamma = \gamma' = 1\tfrac{1}{4}, \quad \delta = 5, \quad \nu = \nu' = \tfrac{9}{14} = 0.6428\ldots,$$

$$\eta = \tfrac{1}{18} = 0.0555\ldots, \quad (d=3). \tag{7.5}$$

The value of γ quoted has been established numerically with considerable certainty,[2b, 39] but the scaling equality $\gamma = \gamma'$ has remained in some doubt.[2b] A recent study by Gaunt and Sykes[40] of the diamond and fcc lattices concludes that the data are not inconsistent with the equality but one must then recognize the presence of additional, weaker singularities in $\chi_0(T)$ below T_c (probably coincident with the critical singularity) which lead to "apparent exponents" with higher values in the range 1.28–1.31. However, Gaunt and Sykes, confirm the value[2b] $\beta \simeq \frac{5}{16}$, which, together with the estimate[2b] of α ($\simeq \frac{1}{8}$) above T_c, confirms scaling and leads to the prediction for δ given in (7.5). This in turn is consistent with the numerical evidence[41] (although earlier analysis[42] suggested a somewhat higher value). The estimates for ν and η are those of I, which were quoted with uncertainties of ±0.0025 and ±0.008, respectively. These values were found consistent with longer series[43] on the bcc and fcc lattices by Fisher and Jasnow.[2c] However, Moore, Jasnow, and Wortis[43, 44] by studying a series of higher and lower moments (including nonintegral orders), concluded that a best overall scaling fit for the fcc lattice could be obtained with a value of ν lower by $\frac{1}{2}$ to 1%. Use of such a lower estimate for ν (and, through scaling, for ν') would lead to amplitude estimates differing from those we find by 1 or 2%, but would not significantly alter our main conclusions.

B. Phase-boundary exponents and amplitudes

On the phase boundary the series for the squared correlation length and the correlation moments become

$$\Lambda_2(u) = [\xi_1(T)/a]^2 = \sum_{n=0}^{\infty} \lambda_{2,n}^{-} u^n, \tag{7.6}$$

$$\mu_t(u) = \sum_{n=0}^{\infty} m_{t,n}^{-} u^n. \tag{7.7}$$

The coefficients $\lambda_{2,n}^{-}$ and $m_{2,n}^{-}$, $m_{4,n}^{-}$ and $m_{6,n}^{-}$ are presented in Tables IV and V.

As is well known, the expansions in u for the sc and bcc lattices do not converge up to the critical point u_c. Consequently, in estimating critical behavior one must rely on Padé approximant techniques.[2b, 45] In particular we have studied Padé approximants to the exponent series

$$2\nu'^*(u) = (u_c - u)(d/du)\ln\Lambda_2(u), \tag{7.8}$$

evaluating at $u = u_c$, which provide estimates for $2\nu'$, and the corresponding estimates for $2\nu' + \gamma'$ obtained from the $\mu_2(u)$ series. Selected diagonal and near diagonal Padé approximants are exhibited in Table VI. From these it is evident that the bcc data are very poorly converged; one can conclude little more than that $2\nu'$ probably lies between 1.2 and 1.4 while $2\nu' + \gamma'$ is between 2.4 and 2.7. Fortunately the sc approximants are more regular and we may conclude

$$2\nu' = 1.285 \pm 20 \quad (\text{sc}), \tag{7.9}$$

$$2\nu' + \gamma' = 2.54 \pm 4 \quad (\text{sc}). \tag{7.10}$$

These values may be compared with the scaling expectations following from (7.5), namely, 1.2857 and 2.5357, respectively. The agreement is good although the uncertainties are significantly larger than above T_c. It is interesting that the estimates (7.9) and (7.10) together indicate a central value $\gamma' \simeq 1.25$ in agreement with scaling, rather than 1.30, which the direct series for χ_0 tend to suggest (as mentioned above). The uncertainties, however, are still rather large.

For the square lattice the series are too short to analyze for ν' and, in any case, there is essentially no doubt that the value $\nu' = 1$ is exact for all moments, especially in the light of the recent analytical work of Barouch, McCoy, and Wu.[46]

Accepting the exponent values (7.4) and (7.5), amplitude estimates may be obtained as usual by evaluating direct Padé approximants to amplitude functions such as

$$m_2^{-*}(u) = (u_c - u)^{2\nu' + \gamma'} \mu_2(u), \tag{7.11}$$

at $u = u_c$. Convergence for the sc lattice is quite good: thus for $m_2^{-*}(u_c)/u_c^5$, sample approximants are [3/3] = 0.4664, [4/4] = 0.4684, [4/5] = 0.4686, [5/4] = 0.4690, [4/6] = 0.4689, [5/5] = 0.4682, [6/4] = 0.4696, from which we adopt the estimate 0.4688

TABLE IV. Coefficients for the expansion of $\Lambda_2(0,T)$ on the phase boundary. (Coefficients of lower order than exhibited vanish identically.)

n	sq $\lambda^-_{2,n+1}$	sc $\lambda^-_{2,n+2}$	bcc $3\lambda^-_{2,n+3}$
0	1	1	4
1	9	−1	−4
2	71	10	0
3	542	−14	56
4	3705	85	−120
5		−169	152
6		884	488
7		−2390	−2096
8		10 212	4308
9		−30 594	1440
10		116 134	−28 008
11			80 868
12			−54 976

± 7. As might be expected, estimates for m_4^- and m_6^- are subject to larger fractional uncertainties. Considering the poor behavior of the bcc exponent estimates, the amplitude estimates are moderately well converged; however, the apparent precision is appreciably worse than for the sc lattice. Despite their shortness, the square lattice series yield estimates of quite good consistency. Corresponding "best" approximants for $\Lambda_2(0, T) = (\xi_1/\alpha)^2$ below T_c are listed in Appendix B.

The resulting estimates for the correlation length amplitudes f_1^-, have already been presented in Table I. The corresponding estimates for m_2^-, m_4^-, and m_6^- are listed in Table VII. Also shown in the table are estimates for m_0^-, which is just the susceptibility amplitude C^-, and the recently calculated exact value for the square lattice.[46] Comparison of the latter with an estimate based on our short series indicates an inaccuracy of about 9% whereas internal evidence suggests an uncertainty of only 4 or 5%. The corresponding values of C^+ are listed in Table I, where the sc and bcc estimates are taken from Sykes *et al.*[38] The ratios C^+/C^- are also shown in Table I; it is interesting to note that the estimates 5.06 and 5.01 for sc and bcc lattices, respectively, are lower than the original estimates of Essam and Fisher[47] (namely 5.40 and 5.19, respectively) and are also in much better agreement with the expectation of universality. (The Essam-Fisher value of 5.14 for the fcc lattice is probably also subject to revision in the light of longer series.[40]) It is evident from the definition (2.12), that the three amplitudes f_1^-, m_0^-, and m_2^- are not independent. Our separate estimates satisfy the required relation to well within the uncertainties quoted.

C. Shape and symmetry of critical scattering

The expansion coefficients $\Sigma_4, \Sigma_6, \ldots$, etc., of the inverse scaling function, $1/\hat{D}(x^2, z)$, defined in (5.26) are a direct measure of how far the scattering line shape differs from a pure Lorentzian form $\hat{D} = (1+x^2)^{-1}$, as predicted by Ornstein-Zernike theories, as the critical point is approached. In terms of the coefficients

$$c_2 = \tfrac{1}{4},\quad c_4 = \tfrac{1}{64},\quad c_6 = \tfrac{1}{2304} \qquad (d=2)\,, \tag{7.12}$$

$$c_2 = \tfrac{1}{6},\quad c_4 = \tfrac{1}{120},\quad c_6 = \tfrac{1}{5040} \qquad (d=3)\,. \tag{7.13}$$

the parameters Σ_4, Σ_6, may be expressed as the limiting critical values of the functions

TABLE V. Expansion coefficients for the correlation moments on the phase boundary. (Coefficients of lower order than exhibited vanish identically.)

	Square			Simple cubic			Body-centered cubic		
n	$m^-_{2,n+3}$	$m^-_{4,n+3}$	$m^-_{6,n+3}$	$m^-_{2,n+5}$	$m^-_{4,n+5}$	$m^-_{6,n+5}$	$3m^-_{2,n+7}$	$9m^-_{4,n+7}$	$27m^-_{6,n+7}$
0	16	16	16	24	24	24	96	288	864
1	272	560	1520	−24	−24	−24	−96	−288	−864
2	3248	11 312	51 632	528	1008	2544	0	0	0
3	32 768	169 088	1 146 752	−960	−1824	−4704	2880	16 320	122 688
4	299 072	2 124 992	19 797 824	8496	23 952	94 032	−6144	−33 792	−248 832
5				−21 312	−59 712	−238 464	5376	26 304	170 304
6				125 904	460 848	2 417 520	57 408	500 160	5 694 096
7				−380 016	−1 401 168	−7 496 016	−200 064	−1 640 064	−18 824 064
8				1 813 416	8 059 080	52 263 240	318 720	2 449 920	26 273 280
9				−6 046 440	−27 451 752	−182 890 536	758 496	9 944 640	173 798 208
10				25 675 200	133 273 248	1 021 855 392	−4 698 048	−52 186 176	−824 103 360
11							10 947 744	114 527 712	1 712 345 760
12							1 699 776	92 047 680	2 854 380 480

$$\Sigma_4(H, T) = \frac{c_4\mu_4(H, T)}{c_2\mu_2(H, T)\Lambda_2(H, T)} - 1\,, \tag{7.14}$$

$$\Sigma_6(H, T) = \frac{c_6\mu_6(H, T)}{c_2\mu_2(H, T)\Lambda_2^2(H, T)} - 2\Sigma_4(H, T) - 1\,. \tag{7.15}$$

In principle, it follows that Σ_4^- and Σ_6^- can be estimated from the values of f_1^-, m_2^-, m_4^-, and m_6^-. However, it is found that Σ_4 (and even more so, Σ_6) are of such a small magnitude as to be significantly smaller than the cumulative uncertainties coming from the original amplitude estimates. Accordingly series were formed directly for $\Sigma_4(0, T)$ and $\Sigma_6(0, T)$ below T_c. Various direct Padé approximants to these series for the sc lattice are shown in Figs. 1(a) and 1(b). The convergence away from T_c is quite good but the functions decrease so rapidly as $T \to T_c$ that the resulting fractional uncertainties are still very large. For the bcc and square lattices the convergence is much less satisfactory. Nevertheless, rough estimates of Σ_4^- may be made. These estimates are collected in Table VIII together with the values of Σ_4^+ and Σ_6^+ following from the approximants developed in Parts I and II for the critical isochore [but *not* based on direct series extrapolation of $\Sigma_4(0, T)$, etc.]. Also included are estimates made below for Σ_4^c. Within the uncertainties, the figures for bcc and sc lattices are consistent with the expectations of universality, i.e., lattice independence. However, the central bcc estimate for Σ_4^- is of opposite sign to that for the sc lattice! In view of the large bcc uncertainties we discount this sign difference. The variation above T_c represents a slight apparant lack of universality in the scattering approximant parameter ϕ_c introduced in I [see (5.29) above]. Despite the large uncertainties it seems clear that the deviations from Lorentzian behavior on the phase boundary (and critical isotherm) are an order of magnitude larger than above T_c on the critical isochore.

According to general scaling ideas the scattering intensity should become spherically symmetric in momentum space (or in real space) as the critical point is approached, despite the anisotropy imposed by the lattice structure outside the critical region. In I this point was investigated above T_c by examining suitable ratios of the expansion coefficients of the Cartesian correlation moments

$$\mu_{f,g,h}(H, T) = \sum_{\vec{R}} (x/a)^f (y/a)^g (z/a)^h \Gamma(\vec{R}, H, T)\,, \tag{7.16}$$

where $\vec{R} = (x, y, z)$. An alternative approach adopted here is to examine these moments as a function of temperature (for $H = 0$). More specifically we define the scattering symmetry ratios

$$\mathcal{S}(f, g, h) = \mu_{f,g,h}(H, T)/\mu_{f+g+h}(H, T)\sigma^0(f, g, h)\,, \tag{7.17}$$

where, in terms of the gamma function $\Gamma(z)$, we have

$$\sigma^0(f, g, h) = \frac{\Gamma(\frac{1}{2}f + \frac{1}{2})\Gamma(\frac{1}{2}g + \frac{1}{2})\Gamma(\frac{1}{2}h + \frac{1}{2})}{2\pi\Gamma(\frac{1}{2}f + \frac{1}{2}g + \frac{1}{2}h + 1\frac{1}{2})}\,. \tag{7.18}$$

The normalization of $\mathcal{S}(f, g, h)$ is such that the ratio has the value unity for any spherically symmetric correlation function. (We restrict attention to three dimensions since exact results are available which confirm isotropy for the square lattice.[2b, 46]

In Fig. 2 some direct Padé approximants to the expansions of various symmetry ratios are plotted for the sc lattice from 30% below T_c to 30% above T_c. Above the critical point all the ratios converge rapidly to unity as $T \to T_c$ so confirming the expected isotropy. Indeed the critical point estimates deviate by only 0.3% or less. Below T_c the situation is similar: apart from the (6, 0, 0) ratio, (which is probably inaccurate close to T_c) the con-

TABLE VI. Estimation of $2\nu'$ and $2\nu' + \gamma'$ for sc and bcc lattices.

Simple cubic			Body-centered cubic		
[L/M]	$2\nu'$	$2\nu'+\gamma'$	[L/M]	$2\nu'$	$2\nu'+\gamma'$
[1/1]	1.290	2.741	[2/2]	1.176	2.526
[2/2]	1.2998	2.1104	[3/3]	1.3268	2.2423
[3/3]	1.1935	2.5243	[4/4]	1.2144	2.0326
[3/4]	1.2562	2.5312	[4/6]	1.2267	2.3814
[4/3]	1.2397	2.5310	[5/5]	1.1987	2.0368
[3/5]	1.2936	2.5484	[6/4]	1.3356	2.3717
[4/4]	(−7.014)	2.5215	[4/7]	1.4050	2.7125
[5/3]	1.2838	2.5495	[5/6]	1.1524	2.4296
[4/5]	1.3009	2.4646	[6/5]	1.0207	2.4259
[5/4]	1.2842	2.4548	[7/4]	1.8758	2.6756
[6/3]	1.2842	2.5691			

TABLE VII. Amplitudes on the phase boundary.

	sq	sc	bcc
$m_0^- = C^-$	0.025 536 9...	0.209 ±0.003	0.197 ±0.002
m_2^-	0.003 24 ±0.000 08	0.071 49 ±0.0001	0.0599 ±0.0006
m_4^-	0.003 58 ±0.0004	0.0876 ±0.002	0.064 ±0.001
m_6^-		0.225 ±0.012	

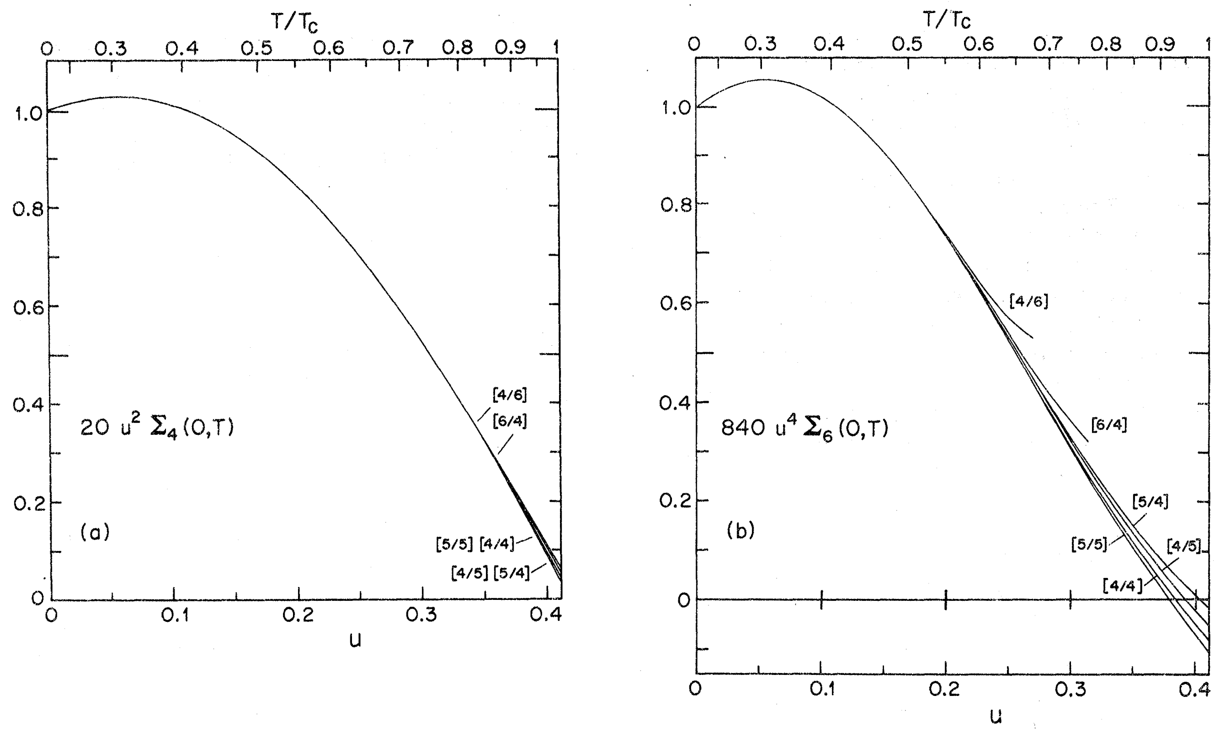

FIG. 1. Variation of (a) $\Sigma_4(0,T)$ and (b) $\Sigma_6(0,T)$ below T_c for the sc lattice according to various Padé approximants, indicating the deviations from Lorentzian line shape.

vergence to unity is within 0.6%. However, it is notable that the growth of asymmetry away from T_c is much more rapid below T_c, an aspect of the scattering which should be susceptible to experimental test.

D. Strong scaling in zero field

As explained in Sec. V B, the correlation function in zero field for fixed $\vec{R}$ (or its Fourier transform at fixed $\vec{k}$) is expected[22-25] to exhibit a singular variation of the form $|t|^{1-\alpha}$ as $T \to T_c$. In accord with scaling, we may take the specific-heat exponents in three dimensions as $\alpha = \alpha' = \frac{1}{8}$. Following Part I we thus write for below T_c

$$\langle s_0^z s_{\vec{R}}^z \rangle \approx \Gamma_c(\vec{R}) + E^-(\vec{R})\,|t|^{1-\alpha'} + \cdots . \tag{7.19}$$

(Note that no contribution of the form $|t|^{2\beta}$ should appear although at first sight one might be expected: this can indeed be checked explicitly for the two-dimensional Ising models where $|t|^{1-\alpha'}$ should, of course, become $t \ln |t|^{-1}$.) According to the strong scaling hypotheses[2b, 22-25] the amplitudes $E^-(\vec{R})$ should vary as

$$E^-(\vec{R}) \approx E_0^-(R/a)^{\zeta} \quad \text{as } (R/a) \to \infty , \tag{7.20}$$

with the relation

$$\zeta = (1-\alpha)/\nu - d + 2 - \eta . \tag{7.21}$$

Using our accepted exponent values predicts $\zeta \simeq 0.3056$ for $d = 3$. Completely analogous conclusions naturally hold above T_c where the point was first investigated in detail by Ferer *et al.*[48] From an analysis of the fcc series for $\langle s_0^z s_{\vec{R}}^z \rangle = \Gamma(\vec{R})$ for (R/a) values up to $\sqrt{11}$ they concluded that $\zeta = 0.47 \pm 0.06$. This is apparently at variance with the strong scaling prediction (7.21).

To study the question below T_c we have formed direct Padé approximants to the series for

$$\mathcal{E}(\vec{R}, T) = \frac{d}{dt} \langle s_0^z s_{\vec{R}}^z \rangle \Big/ \frac{d}{dt} \langle s_0^z s_{\vec{\delta}}^z \rangle . \tag{7.22}$$

The differentiation removes the constant term in

TABLE VIII. Parameters Σ_{2k} measuring deviation from Lorentzian line shape.

	Σ_4^+	Σ_4^-	Σ_4^c	Σ_6^+	Σ_6^-
sq	0.000108	0.13 $\pm$0.07	0.075 $\pm$0.020	-5.25×10^{-6}	
sc	0.00055 $\pm$0.00015	0.013 $\pm$0.005	0.039 $\pm$0.005	$(-5\pm 2)\times 10^{-6}$	-0.007 $\pm$0.003
bcc	0.00071 $\pm$0.00015	-0.016 $\pm$0.030	-0.017 $\pm$0.020	$(-9\pm 3)\times 10^{-6}$	

(7.20) and so, as $T \to T_c$, this function should approach the ratio $E^-(\vec{R})/E^-(\vec{\delta})$. In fact, we find the apparent convergence for $\mathcal{E}_c(\vec{R})$ surprizingly good up to $(R/a)=\sqrt{13}$. (The technique may also be tested above T_c.)

Our detailed findings will be reported elsewhere.[49] The main point is that it is unreasonable in any test of scaling not to allow for some corrections to the expected asymptotic form; this is particularly important when, as in the present case with (R/a), the accessible range of the variable is restricted. On making such allowance[49] we find, in fact, that the data both above and below T_c are consistent with the strong scaling prediction (7.21). We content ourselves here with reporting that if we adopt the estimate[50]

$$E^-(\vec{\delta}) = 3.16 \pm 0.18 \quad (\text{sc}), \tag{7.23}$$

which simply reflects the amplitude of the specific-heat singularity, we find for the amplitude in (7.20) the result

$$E_0^- = 3.91 \pm 0.25 \quad (\text{sc}). \tag{7.24}$$

Together with the amplitude data in Table I this leads to the estimate

$$\tilde{D}^-_{\infty,1}/\tilde{D}^-_\infty = -0.99 \pm 0.07 \quad (d=3), \tag{7.25}$$

for the corresponding scaling function coefficients defined in (5.27). The ratio $\tilde{D}^+_{\infty,1}/\tilde{D}$ may likewise be estimated as 1.74 ± 5 which compares satisfactorily[49] with the recent ϵ-expansion calculation of Fisher and Aharony.[22]

E. True range of correlation

As indicated in Sec. II D the true range of correlation $\xi_{\vec{e}}$ in direction $\vec{e}$ may be found from the location of the singularity of $\Gamma(k\vec{e})$ which lies nearest the real k axis. This singularity is generally expected to be a simple pole.[2] Accordingly, we expect $\kappa_{\vec{e}} = 1/\xi_{\vec{e}}$ to be given by the closest zero of the equation

$$[\bar{\Gamma}(k\vec{e})]^{-1} = \mathcal{C}(k\vec{e}) = 0. \tag{7.26}$$

This can be written

$$\mathcal{C}(\vec{0}) + \sum_{\vec{R}\neq 0} \cosh[\kappa_{\vec{e}}(\vec{e}\cdot\vec{R})]\mathcal{C}(\vec{R}) = 0, \tag{7.27}$$

which, in terms of the truncated (u, y) expansion, can be expressed as

$$\sum_{n=0}^{N} a_n(u, y)(\cosh\kappa_{\vec{e}}a)^n = 0, \tag{7.28}$$

with

$$a_n(u, y) = \sum_{i=0}^{I} \sum_{j=0}^{J} a_{nij} u^i y^j, \tag{7.29}$$

where the upper limits I, J, and N clearly depend on the number of available terms of the $\mathcal{C}(\vec{R})$ expansion. Quite generally for Ising models, the only nonzero coefficient of the form a_{n00} is a_{000}. This means that the expansion for $\cosh\kappa_{\vec{e}}a$ is of the form

$$w = u^{i^0} y^{j^0} \cosh\kappa_{\vec{e}}a = \sum_{i=0} \sum_{j=0} b_{ij} u^{gi} y^{hj}, \tag{7.30}$$

with $b_{00} \neq 0$. The exponents i^0, j^0, g, and h, depend on $\vec{e}$ and on the lattice and are in general nonintegral. The equation determining $\kappa_{\vec{e}}$ may finally be written

$$\sum_{n=0} u^{-i^0 n} y^{-j^0 n} a_n(u, y) w^n = 0. \tag{7.31}$$

This can be solved iteratively to determine the coefficients b_{ij} in (7.30). By way of illustration of the form of the expansion, we mention that $g=h=1$ for (1, 0, 0), (1, 1, 0), and (1, 1, 1) directions on the sc lattice, and for the (1, 0, 0) direction on the bcc lattice. However, for the square lattice $g=\frac{1}{2}$ and $h=1$ for both (1, 0) and (1, 1) directions, while for the (1, 1, 1) direction on the bcc lattice $g=1$, and $h=\frac{1}{3}$.

To determine the number of terms in the (u, y) expansion of the effective reduced second moment $\Lambda_2'(\vec{e}; H, T)$ [defined in terms of $\cosh\kappa_{\vec{e}}a$ through (2.15)] that can be found from a given number of terms of the expansion $\mathcal{C}(\vec{R})$ is a little tricky. In practice this is best determined by careful inspection. Part of the difficulty is that below T_c there is no clear-cut graphical prescription for expanding $\mathcal{C}(\vec{R})$.

We have derived the effective reduced second moment series in zero field on the sc lattice for the two directions

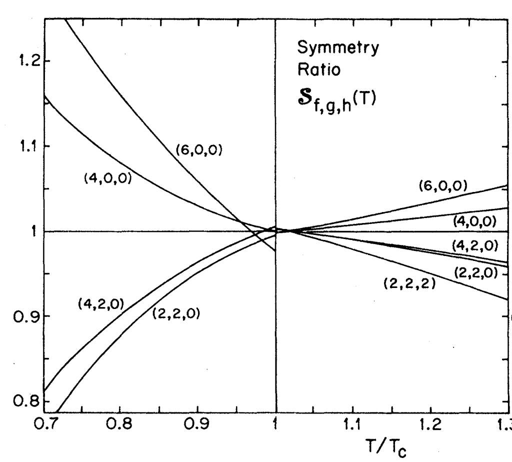

FIG. 2. Padé approximant estimates for symmetry ratios for scattering from the simple-cubic lattice.

$$\vec{e}_0 = (1, 0, 0) \quad \text{and} \quad \vec{e}_1 = (1, 1, 0)/\sqrt{2} \tag{7.32}$$

with the results

$$\Lambda_2'(\vec{e}_0; 0, T) = u^2 - u^3 + 10u^4 - 14u^5 + 93u^6 - 201u^7 + \cdots \tag{7.33}$$

and

$$\Lambda_2'(\vec{e}_1; 0, T) = u^2 - \tfrac{3}{4}u^3 + 9\tfrac{7}{16}u^4 - 13\tfrac{11}{32}u^5 + \cdots . \tag{7.34}$$

By comparison with the data in Table IV one sees that Λ_2' for the axis direction $\vec{e}_0$, is identical to Λ_2 up to order u^5, which is the fourth nonzero term. (It also agrees up to order y^3 in the field expansion.) By contrast the corresponding expansions above T_c in powers of $v = \tanh K$, agree up to order v^8, the ninth term. (See Sec. 8.3 of I.) Furthermore, the coefficient of v^9 in Λ_2' differs by less than 0.01% from that in Λ_2. This indicates, as concluded in I, that the true and second moment correlation lengths are almost identical in magnitude in the critical region above T_c. Below T_c, however, the coefficients of u^6 in Λ_2 and Λ_2' already differ by 10%, while those of u^7 differ by 19%. Correspondingly, we must expect the ratio $\xi_{\vec{e}}/\xi_1 \approx f/f_1$ to deviate more significantly from unity below the critical point. Since there are only two nonzero terms in the difference $\Lambda_2' - \Lambda_2$, we cannot estimate the ratio with any real conviction. However, if we use the approximant $\Lambda_2'/\Lambda_2 = 1 + 8u^5/(1+3u)$ we find $f^-/f_1^- \simeq 1.02$. This agrees better than could be expected with the estimate following from the overall approximants to the scattering developed below (see Sec. VIII).

F. Critical isotherm exponents

The series for the square correlation length and the correlation moments on the critical isotherm can be obtained by setting $u = u_c$ in (6.1) which leads to

$$\Lambda_2(y) = [\xi_1(H)/a]^2 = \sum_{n=1}^{\infty} \lambda_{2,n}^c y^n , \tag{7.35}$$

$$\mu_t(y) = \sum_{n=2}^{\infty} m_{t,n}^c y^n . \tag{7.36}$$

The coefficients $\lambda_{2,n}^c$ and $m_{2,n}^c$, $m_{4,n}^c$, and $m_{6,n}^c$ are presented in Tables IX and X. Since the series in powers of y for all ferromagnetic Ising lattices converge right up to the critical value $y = 1$, it is possible to apply both ratio and Padé approximant techniques in the analysis of the series. Among the former we have used a method of Gaunt to estimate exponents, and a new method, described in Sec. VII G, to estimate amplitudes and the exponent of the leading confluent correction singularity. As we will see, various competing singularities play a dominant role in the extrapolation of the series on the critical isotherm.

Direct plots of the ratios $\mu_n\{\Lambda_2^c\} = \lambda_{2,n}^c/\lambda_{2,n-1}^c$ show large oscillations, of the order ±2 to 5% for sc and bcc, and ±20% for the square lattice. Estimates of the exponent $2\nu^c$ based on the linear extrapolants

$$2\nu_n^c = 1 + (n+\epsilon)(\mu_n - 1) , \tag{7.37}$$

for various values of the shift ϵ, lead only to the conclusion that $2\nu^c$ lies between 0.8 and 0.9 in three dimensions. However, use of the means of alternate ratios for the sc lattice suggests 0.84 ± 0.03. By taking the square root of alternate ratios the square lattice series indicate $2\nu^c = 1.00 \pm 0.05$. These rather rough estimates are to be compared with the scaling predictions following from (2.29) and (2.24), namely,

$$2\nu^c = \tfrac{16}{15} = 1.0666\ldots, \quad \gamma^c = \tfrac{14}{15} = 0.9333\ldots, \quad (d=2), \tag{7.38}$$

$$2\nu^c = \tfrac{144}{175} = 0.8228\ldots, \quad \gamma^c = \tfrac{4}{5} = 0.80, \quad (d=3). \tag{7.39}$$

Although not inconsistent with scaling the results are not very encouraging. The ratio plots for the μ_2 series display less oscillation, but for all three lattices the corresponding exponent estimates lie some 5 to 7% above the scaling predictions.

Selected Padé approximants to exponent functions analogous to (7.8) are displayed in Table XI. The results for the square lattice, from which we conclude, say, $2\nu^c = 1.05 \pm 0.02$ and $2\nu^c + \gamma^c = 2.02 \pm 0.04$, are in reasonable agreement with the scaling predictions (7.38) (which yield $2\nu^c + \gamma^c = 2$). However, both the sc and bcc data suggest $2\nu^c = 0.86 \pm 0.01$ which appears to be significantly higher than the scaling prediction. The estimates for $2\nu^c + \gamma^c$ are somewhat more erratic but suggest a value exceeding 1.70, whereas scaling predicts $2\nu^c + \gamma^c \simeq 1.62$.

TABLE IX. Coefficients $\lambda_{2,n}^c$ for the expansion of $\Lambda_2(H, T_c)$ in powers of y.

n	sq $\lambda_{2,n}^c$	sc $\lambda_{2,n}^c$	bcc $3\lambda_{2,n}^c$
1	0.142 136	0.099 804 8	0.282 643
2	0.112 847	0.085 651 8	0.234 055
3	0.142 551	0.085 160 8	0.226 093
4	0.114 514	0.077 246 3	0.209 510
5	0.151 314	0.077 137 5	0.205 512
6	0.114 719	0.073 329 5	0.197 562
7	0.150 398	0.072 543 9	

TABLE X. Expansion coefficients for the correlation moments on the critical isotherm. (Note that $m^c_{l,1} = m^c_{l,0} = 0$.)

	Square			Simple cubic			Body-centered cubic		
n	$m^c_{2,n}$	$m^c_{4,n}$	$m^c_{6,n}$	$m^c_{2,n}$	$m^c_{4,n}$	$m^c_{6,n}$	$3m^c_{2,n}$	$9m^c_{4,n}$	$27m^c_{6,n}$
2	0.066 945	0.066 945	0.066 945	0.167 497	0.167 497	0.167 497	0.546 602	1.639 805	4.919 416
3	0.125 332	0.277 577	0.810 434	0.320 924	0.655 263	1.725 150	0.982 522	6.037 434	47.775 028
4	0.187 572	0.606 531	2.832 318	0.459 546	1.396 593	5.785 198	1.350 348	12.226 037	151.680 924
5	0.243 820	1.067 036	6.750 887	0.583 309	2.350 466	13.158 168	1.677 718	19.843 268	329.598 463
6	0.310 193	1.685 660	13.357 342	0.700 214	3.489 396	24.469 485	1.984 224	28.718 493	591.857 057
7	0.365 815	2.421 330	23.316 07	0.809 035	4.789 143	40.216 609	2.270 141	38.699 102	947.048 991
8	0.430 258	3.326 313	37.547 04	0.913 371	6.240 476	60.847 793			

At first sight these results for $d=3$ seem to indicate a rather clear violation of the exponent relation (2.29) derived from scaling. However, we are not inclined to take them at face value. Gaunt and Sykes,[41] in their study of the magnetization on the critical isotherm, concluded that there were important confluent singularities at the critical point with a rather small, and hence more disturbing, exponent value. We will reach similar conclusions below, for the correlation moments. Such singularities are well known to slow the convergence of Padé approximants and we believe they are the cause of the apparent discrepancy with scaling. To study this issue more closely we return to the ratio approach, which is slightly less sensitive to such singularities.

The existence of the large oscillations in the ratios indicate the presence of strong nonphysical singularities near $y=-1$. This is confirmed by the Dlog Padé analysis, and Gaunt and Sykes[41] observed similar singularities in the magnetization series near $y=-1.25$ for $d=2$, and near $y=-2$ for $d=3$. Such singularities can be removed further from the circle of convergence by application of the Euler transformation

$$w=(1+b)y/(1+by). \tag{7.40}$$

This takes the point $y=1$ to $w=1$ but removes $y=-1$ to $w_{-1}=-(1+b)/(1-b)$. As b increases from 0 to 1, and w_{-1} goes from 0 to $-\infty$, the oscillations in the ratios of the w expansion quickly damp out. In three dimensions the oscillations become quite moderate for $b=\frac{1}{2}$ or $w_{-1}=-3$ and this value was adopted for subsequent analysis. For the square lattice $b=\frac{9}{11}$, or $w_{-1}=-10$, was found satisfactory. Figure 3 shows the estimates of $2\nu^c$ following via (7.37) from the slopes of the corresponding ratio plots for the transformed Λ_2^c series. Note the scaling predictions are marked by an arrow. Evidently the transformed series are consistent with scaling although their behavior is not very regular. One might indeed be tempted to choose a somewhat higher estimate such as

$$2\nu^c=0.835\pm0.020 \quad (d=3). \tag{7.41}$$

There is little point in quoting a similar estimate for $d=2$ since the scaling prediction is almost surely correct there; certainly the data of Fig. 3 give no cause to doubt it. The transformed μ_2^c series for the square lattice again support the scaling prediction $2\nu^c+\gamma^c=2$ within 1%. The transformed μ_2^c series for $d=3$, however, still tend to indicate higher values of $2\nu^c$ but now by only about 3 or 4%. (The Euler transformation has, not unexpectedly, relatively little effect on the Padé approximant analysis.)

The transformed Λ_2^c and μ_2^c series may also be studied by examining the expansion coefficients of the corresponding logarithmic derivatives. Since $y_c=w_c=1$, the coefficients of these series should approach $2\nu^c$ and $2\nu^c+\gamma^c$, respectively. In fact these coefficients vary rather slowly, e.g., for the sc $y(d/dy)\ln\Lambda_2^c$ series, from 0.924 at $n=2$ to 0.863 at $n=6$. This behavior clearly indicates a confluent singularity at $y=y_c=1$. If the exponent of this singularity were known, the coefficient limits could be estimated by plotting versus the appropriate power of $1/n$. Unfortunately, the series themselves do not seem long enough to indicate this reliably without other assumptions (see below). If the coefficients are simply extrapolated versus $1/n$ the exponent estimates obtained again lie 3 or 4% above the scaling predictions.

TABLE XI. Selected Padé approximant estimates of exponents on the critical isotherm.

	Square		Simple cubic		Body-centered cubic	
$[L/M]$	$2\nu^c$	$2\nu^c+\gamma^c$	$2\nu^c$	$2\nu^c+\gamma^c$	$2\nu^c$	$2\nu^c+\gamma^c$
[1/1]	1.0307	1.9617	0.8967	3.7784	0.8659	1.6905
[1/2]	1.0402	1.9956	0.8617	1.7608	0.8551	1.7077
[2/1]	1.0401	1.9941	0.8583	1.7555	0.8547	1.7054
[2/2]	1.0279	1.9174	0.8637	1.7435	0.8560	1.7122
[1/3]	1.0849	2.0734	0.8639	1.7494	0.8561	1.7128
[3/1]	1.0835	2.0672	0.8650	1.7461	0.8562	1.7133
[2/3]	1.0555	2.0286	0.8626	1.6888		
[3/2]	1.0545	2.0256	0.8619	1.7461		

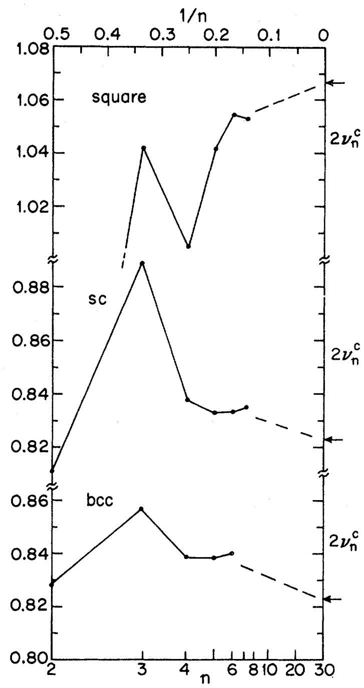

FIG. 3. Estimates of $2\nu^c$ following from ratios of the transformed Λ_2^c series (a) for the square lattice and (b) for sc and bcc lattices with $\epsilon = 0$. The scaling predictions are marked by an arrow.

To summarize the results of these investigations, it must be concluded (i) that scaling is confirmed in two dimensions but (ii) that most straightforward methods of analysis suggest values of $2\nu^c$ and $2\nu^c + \gamma^c$ for $d = 3$ which somewhat exceed the scaling predictions even though certain ratio methods applied to the Λ_2^c series are quite consistent with scaling. However, the discrepancies between the various approaches, and the evidence for the presence of confluent singularities, lead us to believe that the inconsistencies with scaling should not be taken very seriously. In addition, it must be noted that the present series are not very long. Similar length series for the magnetization originally lead to the estimate[42] $\delta \simeq 5.2$ whereas longer series obtained later[41,51] lead to $\delta \simeq 5$, a change of 4%.

G. Amplitudes on the critical isotherm

In estimating amplitudes on the critical isotherm we will, as below T_c, assume the exponent values predicted by scaling, given now in (7.38) and (7.39). The amplitudes f_1^c and m_t^c have been estimated by forming direct Padé approximants to the series $(1-y)(\Lambda_2^c/y)^{1/2\nu^c}$, $(1-y)^{2\nu^c}\Lambda_2^c/y$, $(1-y)^{p\nu^c+\gamma^c}\,\mu_p^c/y$, and $(1-y)(\mu_p^c/y^2)^{1/(p\nu^c+\gamma^c)}$. The resulting estimates are displayed in Table XII (where the uncertainties quoted refer to the last decimal place). The convergence of the approximants is not very good as is indicated by the comparatively large uncertainties shown (which, of course, refer *only* to the apparent consistency of the extrapolations and take no account of other sources of inaccuracy). The appearance in many of the Padé approximants of close zero-pole pairs located near $y = 1$ is also indicative of the confluent singularities discussed above.

A check on the reliability of the amplitude estimates for $\Lambda_2^c(H)$ and $\mu_2^c(H)$ can be made via the relations (2.12) and (2.13) which imply

$$m_2^c = 2dC^c(f_1^c)^2 . \qquad (7.42)$$

Gaunt[41,51] has provided careful direct estimates of the amplitude C^c on the basis of longer series for $\chi_0 = \mu_0$ than available for Λ_2^c and μ_2^c. These estimates, which have a precision of better than 1%, (see Table I), may be compared with values calculated through (7.42) from m_2^c and f_1^c. In fact, the values found from our Padé estimates fall some 3, 8, and 6% below the direct estimates for the square, sc, and bcc lattices, respectively. These large deviations cannot be considered satisfactory; they are, presumably, just another indication of the disturbing influence of the confluent singularities. We turn now to an alternative technique which specifically allows for such singularities.

The expected asymptotic forms for $\xi_1^c(H)$ and $\mu_p^c(H)$ as $H \to 0$ may be written

$$\xi_1(H, T_c) \approx f_1^c a |h|^{-\nu^c}(1 - e_1^c |h|^{\rho} + \cdots) , \qquad (7.43)$$

$$\mu_p(H, T_c) \approx m_p^c |h|^{-p\nu^c - \gamma^c}(1 - l_p^c |h|^{\sigma_p} + \cdots) , \qquad (7.44)$$

where ρ and σ_p denote the exponents of the singular corrections. On the grounds of universality one would expect $\rho = \sigma_p$ (all p) and this will indeed be confirmed numerically. In the case $p = 0$ such a singular correction has already been noticed by Gaunt and Sykes,[41] in the susceptibility $\chi_0 = \mu_0$. They argued for the relation $\sigma_0 = 1 - (1/\delta)$ ($= 0.8$ for $d = 3$); however, σ_0 could well be a distinct

TABLE XII. Summary of initial Padé approximant estimates of amplitudes on the critical isotherm. (The uncertainties quoted are in the last decimal place.)

Lattice	f_1^c	m_2^c	m_4^c	m_6^c
sq	0.235 ± 2	0.0151 ± 1	0.0147 ± 2	0.030 ± 1
sc	0.2545 ± 5	0.0927 ± 8	0.118 ± 5	0.29 ± 3
bcc	0.239 ± 2	0.081 ± 4	0.091 ± 3	0.21 ± 2

TABLE XIII. Amplitudes and higher-order correction parameters on the critical isotherm. (The uncertainties quoted refer to the last decimal place.)

Lattice	f_1^c	e_1^c	ρ	m_2^c	l_2^c	σ_2
sq	0.233 ± 1			$0.01537\pm\ 8$		
sc	0.257 ± 2	0.56^{+20}_{-10}	0.77 ± 7	$0.0997\ \ \pm20$	3.6^{+8}_{-4}	0.77 ± 7
bcc	0.242 ± 2	0.40^{+20}_{-10}	0.77 ± 7	$0.0851\ \ \pm20$	2.1^{+10}_{-5}	0.77 ± 7

"correction-to-scaling exponent."

Various methods may be envisaged to obtain estimates of ρ, σ_p, e_1^c, l_p^c, f_1^c, and m_p^c *given* the (assumed) values of the dominant exponents ν^c and γ^c. We have proceeded by forming the series

$$y[\Lambda_2(H,T_c)/y]^{1/2\nu^c}=\sum_{n=1}^{\infty} d_n y^n\,, \tag{7.45}$$

which behaves like $(\xi_1^c)^{1/\nu^c}\sim|h|^{-1}$ [and, analogously, $(\mu_2/y^2)^{1/(2\nu^c+\gamma^c)}$]. Then, by substituting $|h|\approx\frac{1}{2}(1-y)$ as $H\to0+$ in (7.43), and using the binomial theorem to expand in powers of y, we see that for large n the coefficients d_n are expected to vary as

$$d_n\approx 2(f_1^c)^{1/\nu^c}\{1-[e_1^c/2^\rho\nu^c\Gamma(1-\rho)]n^{-\rho}+\cdots\}\,. \tag{7.46}$$

Accordingly, a plot of d_n vs $1/n^\rho$ should approach linearity with a slope proportional to e_1^c and an intercept $2(f_1^c)^{1/\nu^c}$ at $n=\infty$.

One may now plot d_n against various trial powers of $1/n$ and select the most linear graph to determine ρ, f_1^c, and e_1^c. The estimates for f_1^c and analogously m_2^c obtained this way are an improvement over the Padé results and yield estimates for C^c through (7.42) in better agreement with Gaunt's results. Better results are obtainable, however, by an iterative method in which one starts with a first estimate of f_1^c, obtained, say, from the direct Padé approximants. One may then form the differences

$$c_n=d_n-2(f_1^c)^{1/\nu^c}\,, \tag{7.47}$$

or, strictly, estimates for them. By (7.46) the ratios of these differences should behave as

$$c_n/c_{n-1}\approx 1-\rho/n+\cdots\,. \tag{7.48}$$

A plot of these ratios versus $1/n$ thus leads to a (first) estimate for ρ. Armed with this, a plot of d_n vs $1/n^\rho$ leads to an improved estimate of f_1^c and the cycle can be repeated.

In practice we have worked with the Euler transformed series for Λ_2^c and μ_p^c as discussed in the previous section. This reduces the effects of the oscillations. The initial ratio plots of the c_n/c_{n-1} are usually distinctly nonlinear so that only a rough estimate of ρ (or σ_p) is possible. However, after one or two more iterations good convergence is obtained for the sc and bcc lattices with surprizingly linear final plots of d_n vs $1/n^\rho$. The results obtained are listed in Table XIII. The differences from the Padé estimates are appreciable in m_2^c and in m_4^c. (The series for m_6^c are too irregular to justify the detailed analysis.) The derived values of C^c for the three-dimensional lattices are still lower than the linear estimate but only by 3 or 4% which is well within the cumulative uncertainties.

Although the uncertainties in the estimation of the exponents ρ and σ_2 for $d=3$ are considerable, the expectations of universality are confirmed both with regard to lattice structure and to different dependent function. The amplitudes e_1^c and l_2^c are of similar magnitude on both sc and bcc lattices but are not, of course, expected to be universal. The large errors quoted for these amplitudes arise from the fact that, through (7.46), the estimates depend on the factors $\Gamma(1-\rho)$ and $\Gamma(1-\sigma_2)$ which vary, very rapidly, for ρ and σ_2 near 1. Thus the uncertainties in the estimates of ρ and σ_2 propagate strongly into the estimates for e_1^c and l_1^c.

The above procedures could not be applied to the square lattice because the low-order terms are too irregular. However, estimates of the leading singularities could be obtained by plotting the coefficients of $(\Lambda_2/w)^{1/\nu^c}$ and $(\mu_2/w^2)^{1/(2\nu^c+\gamma^c)}$ in the transformed series versus $1/n$; the last few points on the plot show a clear trend which can be extrapolated to $n=\infty$ with reasonable confidence. In fact, as can be seen from Table XIII, the agreement with Gaunt's estimates for C^c is now within 0.25% which is most satisfactory. (However, no estimates of ρ, σ_2, e_1^c, or l_1^c can be quoted.)

Closed-form approximants for $\Lambda_2(H,T_c)$ and $\mu_2(H,T_c)$, etc., can readily be constructed from (7.45), (7.46), and (7.43) by standard ratio techniques.[2b] Formulas for $\Lambda_2(H,T_c)$ on all three lattices are given in Appendix B.

Finally, we have used the method explained in Sec. VII C to estimate the limiting shape parameter Σ_4^c on the critical isotherm. The results for the three lattices have already been presented in

Table VIII. It should be borne in mind, however, that the Padé methods used do not allow for any confluent singularities in $\Sigma_4(H, T_c)$ as $H \to 0$.

H. Amplitudes above T_c

The critical points (7.2) and (7.3) adopted in this work for the sc and bcc lattices are taken from the work of Sykes, Gaunt, Roberts, and Wyles[38b] and are based on the analysis of high-temperature-series expansions of great length (to orders v^{17} and v^{15} for the sc and bcc lattices, respectively). These estimates differ from those used in Part I by only 9 parts in 10^5 and 2 parts in 10^4 for the sc and bcc, respectively. However, use of the revised critical point estimates would lead to some changes in the estimates given in I. While we may still adopt the same critical point exponents (as we have done) the various amplitude estimates will be subject to some corresponding revision. Accordingly in Table I we have quoted for C^+ on the sc and bcc lattices the estimates appearing in the published paper by Sykes *et al.*,[38b] which are 0.2% and 0.5%, lower than the values implied (but not explicitly stated) in I. We must expect that the corresponding estimates of the amplitudes $(f_1^+)^{2-\eta}$ for $\xi_1^{2-\eta}$, which is asymptotically proportional to $\chi_0(T)$, will be modified in a closely similar way. Thus the value quoted in Table I for f_1^+ are not those implied directly by I (by taking F_1^{-1}) but are rather calculated by assuming that the values of the ratio

$$\lim_{T\to T_c+} \frac{(\xi_1 a)^{2-\eta}}{\chi_0} = \frac{(f_1^+)^{2-\eta}}{C^+} = \left(\frac{r_1}{a}\right)_c^{2-\eta}, \tag{7.49}$$

remain the same as quoted in I (in Table VII). While it would in principle be preferable to re-extrapolate the high-temperature series using the new critical points, the changes in the estimates of f_1^+ amount only to 0.1% and 0.27% and are, in any case, just about at the level of precision of the estimates. Any changes due to re-extrapolation are thus almost certain to lie well within the intrinsic uncertainties.

Since the universal ratio Q_3 defined in (5.23) involves precisely the ratio (7.49) the values quoted in Table I follow from I with the revised estimates of $\hat{D}$ presented in II. Thus the values of the scaling function parameter ϕ_c remain those found in II.

Unfortunately, it came to our notice after the bulk of our calculations were completed that Sykes *et al*[38b] had subsequently revised their estimates of C^+ downwards by a further 0.02% and 0.07% for sc and bcc lattices, respectively. [The revised figures were presented in the "reprints" of the published journal article. However, for consistency with Eqs. (3.18) and (3.19) of the Sykes *et al.* reprint, their Eq. (4.6) should read $A_T = 1.0583$ (sc), 0.9861 (bcc).] The change in the sc estimate would yield almost no differences in any of the figures we have quoted but the revised estimate for the bcc lattices would, if adopted, cause slight changes in some of our results, e.g., in Table II where the parametric equation of state is compared with the Essam-Hunter estimates. However, these latter estimates are in turn subject to revision by virtue of the altered figures for T_c, etc. Furthermore, all changes would remain within the quoted uncertainty limits. Thus it does not seem worthwhile to recompute our estimates for f_1^+, etc., using these latest estimates.

VIII. SCATTERING FUNCTION

In this section we summarize briefly the results found and report on the final expressions for the critical scattering intensity.

A. Summary

The analysis of the series expansions for the correlation function $\Gamma(\vec{R}, H, T)$ has lead to checks on the exponent values predicted by scaling. [See Sec. II E and (7.4) and (7.5).] In particular the relation $\nu = \nu'$ was confirmed to within 2% for the sc lattice. The bcc and square lattice data yield less precision but are also consistent. Most direct estimates on the critical isotherm in three dimensions yield estimates some 3 or 4% higher than the prediction $\nu^c = \nu/\beta\delta$. More detailed analysis, however, reveals the presence of important confluent singularities (Secs. VII F and VII G) which disturb the convergence of simple estimation procedures. It is concluded that the data are not actually inconsistent with the scaling prediction. For the square lattice the scaling relation for ν^c is verified to within 1%.

Accepting the scaling predictions for the exponents [specifically with $\nu = \nu' = \frac{9}{14}$ and $\eta = \frac{1}{18}$ in three dimensions; see (7.4) and (7.5)] estimates of critical amplitudes were obtained on the phase boundary below T_c and on the critical isochore. Most of the amplitudes (which are defined in Sec. II E) are listed in Table I. Explicit approximants for the reduced susceptibility or zero angle scattering $\chi_0(H, T)$, and for the second moment correlation length $\xi_1(H, T)$, on the three basic critical loci are listed in Appendix B. The expressions given there for the critical isotherm also take account of the confluent critical singularities, already mentioned, which play a significant numerical role outside the immediate critical vicinity.

The estimate for the critical amplitudes enable one to test the universality of the scaling functions for the susceptibility, correlation length, and cri-

TABLE XIV. Summary of universal amplitude parameter estimates [see (4.5), (4.21), (5.11), (5.23), Tables I and VIII].

Parameter	$d=2$	$d=3$	Mean field
C^+/C^-	37.693 562	5.03	2
$Q_1 = C^c\delta/(B^{\delta-1}C^+)^{1/\delta}$	0.880 23	0.899	1
f_1^+/f_1^-	3.22	1.96	$\sqrt{2}$
$Q_2 = C^+(f_1^c/f_1^+)^{2-\eta}/C^c$	2.88	1.21	1
$Q_3 = \hat{D}(f_1^+)^{2-\eta}/C^+$	0.413 79	0.899	1
Σ_4^-	0.13	0.0133	0
f^+/f_1^+	1.000 054	1.0003	1
f^-/f_1^-	1.61	1.0069	1
f^c/f_1^c		1.0035	1

tical scattering. Specifically, various amplitude ratios are found (within the uncertainties) to take universal values independent of lattice structure. The estimates adopted for these universal combinations are summarized in Table XIV. (The uncertainties to be attached to these estimates can be gauged from Table I.) Comparison with the mean-field values, also listed in Table XIV, reveals significant differences, many not previously known quantitatively.

The parameters C^+/C^- and Q_1 serve as a check on thermodynamic universality. Through the universal "cubic model" parametric equation of state introduced in Sec. IV [Eqs. (4.6)–(4.9), (4.15), (4.17), (4.19), (4.20) and Table III], one can then derive the asymptotic behavior of $\chi_0(H, T)$ in the whole critical region; tests of this representation of the equation of state against previous estimates for higher field derivatives are very encouraging.

The parameters f_1^+/f_1^- and Q_2 likewise provide a check on the universality of the second moment correlation length $\xi_1(H, T)$. This, in turn, can then be represented asymptotically throughout the critical region by using the cubic equation of state and the quartic parametric form (5.9) with constants given in (5.3) and (5.12). While detailed tests of the field dependence have not been performed we believe the accuracy of this representation should be good.

The scattering intensity $I(\vec{k})$ relative to the noninteracting intensity $I_0(\vec{k})$ can, restating the conclusion of Sec. V B, now be written asymptotically in the scaling form

$$I(\vec{k})/I_0(\vec{k}) = \hat{\Gamma}(\vec{k}, H, T) \approx \chi_0(H, T)\hat{D}(x^2, z), \tag{8.1}$$

as $T \to T_c$, $H \to 0$, and $ka \to 0$, with scaling variables

$$x = k\xi_1(H, T), \quad z = h/|t|^{\beta\delta}, \tag{8.2}$$

where $D(x^2, z)$ is the line-shape scaling function [and $h = mH/k_BT_c$, $t = (T-T_c)/T_c$]. The variable z can equally well (and, in practice, more usefully) be replaced by the parametric variable θ used in the equation of state (specifically, say, in the cubic form referred to above). The parameter Q_3 checks the universality of the line-shape scaling function in the limit of large x. In this limit its behavior is specified by (5.21)–(5.25) with (5.9) and (4.17), in order to reproduce the critical point variation

$$I_c(\vec{k})/I_0(\vec{k}) = \hat{\Gamma}_c(\vec{k}) = \hat{D}/(ka)^{2-\eta}, \quad (ka \to 0). \tag{8.3}$$

The asymptotic spherical symmetry embodied in the dependence only on the scalar variable x was established in Sec. VII C. However it was found that anisotropy in the scattering, reflecting the lattice structure, sets in much more rapidly below T_c than above T_c. For small x the line-shape scaling function varies as

$$\hat{D}(x^2, z) = 1/[1 + x^2 - \Sigma_4(z)x^4 + \cdots]. \tag{8.4}$$

The universality of $\Sigma_4(z)$, which represents the first deviations from the Ornstein-Zernike form, was also tested in Sec. VII C. Although only poor precision is attainable (see Table VIII) one may reasonably adopt, for Σ_4^- below T_c, the values exhibited in Table XIV.

The accuracy of the representation (8.1) outside the immediate critical region [i.e., for finite $(T-T_c)$, H, and $\vec{k}$,] may be improved by replacing k in the definition (8.2) of x by the effective, lattice-dependent wave vector $K(\vec{k})$ defined in Part I Eq. (2.2). However, for higher accuracy, further field- and temperature-dependent modifications would be needed to $\hat{D}(x^2, z)$, which have not been studied here. (See I for results above T_c with $H=0$.) The form of the scaling function $\hat{D}(x^2, z)$ was discussed in further detail in Secs. V B and V C. We turn now to the application of the approximants suggested there.

B. Scattering approximants for three dimensions

The preferred approximant for the three-dimensional lattices is, restating (5.38),

$$\hat{D}_B(x^2, \theta) = \frac{(1+\phi^2x^2)^{\eta/2}}{1+\psi x^2} \times\left[1 - \lambda + \lambda\frac{1+\frac{1}{4}\psi x^2}{2\ln\omega}\ln\left(\frac{\omega^2+\frac{1}{4}\psi x^2}{1+\frac{1}{4}\psi x^2}\right)\right]. \tag{8.5}$$

The parameters ϕ, λ, and ω are to be universal functions of θ (or equivalently of $z = h/|t|^{\beta\delta}$), in terms of which $\psi(\theta)$ is given explicitly by (5.39) [which ensures the small x normalization implied by (8.4)]. In addition, to satisfy (8.3), ϕ, λ, and ω must be related to $\hat{D}_\infty(\theta)$, defined in (5.25) with (5.9) and (4.17), by the expression (5.40); this

TABLE XV. Parameters for scattering approximants in three dimensions [see (8.5)].

$\eta=\frac{1}{18}$, $\phi=0.149$, $\omega^2=18.288$, $\psi(\theta)=1.000\,62/[1-0.168\,68\lambda(\theta)]$.

θ	0	0.2	0.4	0.6	$\theta_c=0.8224$	0.85	0.90	0.95	1.0
$h/l_0\lvert t\rvert^{\beta\delta}$	0	0.0422	0.2049	0.7554	∞	13.265	1.9367	0.4870	0
$100\,\lambda(\theta)$	0	0.668	0.4640	1.649	4.481	4.895	5.780	6.702	7.618

equation may be solved explicitly for $\lambda(\theta)$. As explained in Sec. V C, the approximant (8.5) displays a dominant pair of poles at $x=\pm i\psi^{-1/2}$ which are always expected to be present. In addition, at the "two-particle" singularities at $\pm 2i\psi^{-1/2}$, the approximant introduces the expected logarithmic type singularity; this, however, should be absent in zero field above T_c, so that we require $\lambda(\theta)\to 0$ as $\theta\to 0$. In this limit (8.5) reduces to the Fisher-Burford (FB) form found to be successful in I. The remaining singularities at $x=\pm i\phi^{-1}$ and $\pm 2i\omega\psi^{-1/2}$, should lie no closer to the real axis than at $\pm 3i\psi^{-1/2}$, and represent, in approximation, the infinite set of "multiparticle" singularities which should occur at $\pm ni\psi^{-1/2}$ with $n=1, 2, 3, \ldots$.

Unfortunately the data derived by series analysis in Sec. VII are not nearly extensive enough or sufficiently accurate to warrant the full freedom remaining in (8.5). In addition to the value of the exponent η, we may utilize the data for Q_3 and Σ_4^- in Table XIV. One might also use Σ_4^c and Σ_4^+ but these are not known with sufficient independent reliability to be worthwhile. The same applies to Σ_6^-, etc. For this reason, as mentioned in Sec. V C, we will hold ϕ *fixed* at the value required on the critical isochore ($\theta=0$). This should be quite satisfactory since, in any case, owing to the smallness of η the effects on $\hat{D}_B(x^2, \theta)$ of changes in ϕ will be slight. Now consider the remaining parameters λ and ω: one can easily see that the mixing parameter λ must play a major role as θ varies from 0 to 1 since it determines the relative amplitude of the second singularity and can respond directly to the variation of $\tilde{D}(\theta)$ in (5.40). On the other hand the approximant is fairly insensitive to the value of ω. Accordingly we have fitted λ and ω at $\theta=1$ to Σ_4^- as well as $\tilde{D}(\theta)$; then, for general θ, we have held ω fixed at the value found and simply solved (5.40) for $\lambda(\theta)$. The resulting values of ϕ and ω, $\psi(\theta)$, and a short table of $\lambda(\theta)$ are presented in Table XV.

From this table we first note that $\phi^{-1}>6$ and $2\omega>8$, so that the additional weak singularities do indeed lie beyond the "three-particle" branch point. Secondly, from the values of ψ we can obtain, as explained in Sec. II D and V C, estimates for the relative amplitude of the *true* or *exponential range of correlation*. The ratio f/f_1 above T_c is extremely close to unity as already observed in I (although the present numerical estimate for $d=3$ supercedes that reported in I). Below T_c the deviation from unity is an order of magnitude larger, but still amounts to less than 1%. The value found is also in quite reasonable accord with the rough direct estimate, $f^-/f_1^-\simeq 1.02$, made in Sec. VII E. In this connection it must be realized that the deviations of the ratios f/f_1 from unity are, even optimistically, subject to uncertainties of 30 to 40% since they derive numerically rather directly from the corresponding $\Sigma_4(\theta)$ estimates (see Table VIII).

In order to appreciate the nature of the scattering intensity predictions following from (8.5) the

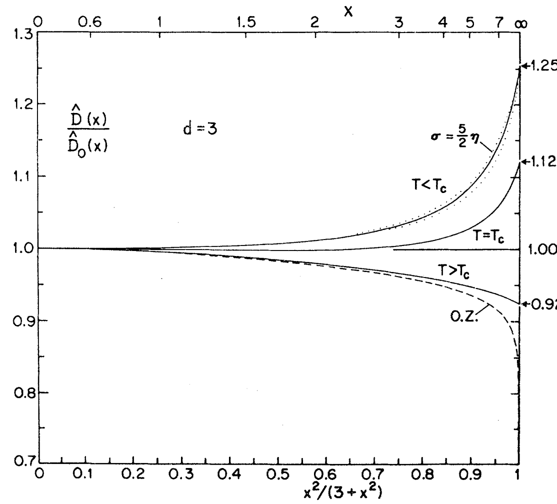

FIG. 4. Plots of approximants for the scaling functions $\hat{D}(x^2)$ for the critical scattering reduced by the zeroth-order approximant $D_0(x^2)=(1+\psi x^2)^{-1+\eta/2}$, on the critical isochore ($T>T_c$), critical isotherm ($T=T_c$), and phase boundary ($T<T_c$), for three-dimensional lattices. The dashed line, which meets the right-hand ordinate axis only at $\hat{D}/\hat{D}_0=0$, represents the Ornstein-Zernike approximation. The dotted curves below T_c derived from the *ad hoc* approximant (5.33) with $\sigma=\frac{3}{2}\eta$ (see text). The variable $x^2/(3+x^2)$ is introduced purely for graphical convenience.

approximant may be normalized by the zeroth order approximant[4] $\hat{D}_0(x^2) = (1+\psi x^2)^{-1+\eta/2}$, which only allows for the nonzero value of η. As evident from Fig. 4 (which supercedes the figure in Ref. 9) the deviations from this, and from the Ornstein-Zernike form (dashed line) become quite significant for $x \gtrsim 2.5$ when $T \leqslant T_c$. By contrast, as noted in I, the OZ approximation in zero field above T_c remains accurate to within 1 or 2% to much greater values of x.

Also shown in Fig. 4 (dotted curves) are the results which follow on the phase boundary from the *ad hoc* approximant $\hat{D}_A(x^2)$ introduced in (5.33), with $(\sigma, \phi', \phi'', \psi') = (\frac{3}{2}\eta, 0.3578, 0.07026, 1.0138)$ and $(\frac{5}{2}\eta, 0.3029, 0.1104, 1.0136)$. These values provide fits to Q_3 and Σ_4^-. The intermediate approximant with $(2\eta, 0.3247, 0.09355, 1.0137)$ cannot be distinguished graphically from our best approximant (8.5). Although the approximant $\hat{D}_A(x^2)$ cannot be considered as satisfactory theoretically as (8.5), the deviations which occur for large but finite x do give some indication of the reliability, or lack thereof, in this region! The discrepancies reflect, of course, the inescapable arbitrariness in the approximants selected. However, one cannot realistically hope to reduce this unless some of the large-x information discussed in Sec. VII D, in relation to the expected $|t|^{1-\alpha}$ singularity in $\hat{\Gamma}(\vec{k}, T)$, can be incorporated into the approximants.

Finally, in Fig. 5 we display plots of the scattering intensity versus T for various fixed momenta on the sc lattice according to (8.1), using Appendix B for χ_0. The main feature, namely, the maximum *above* T_c at nonzero $\vec{k}$ was discovered before, in I, and has been discussed in various places.[22-25] However, it is appreciably less marked in this figure than in Fig. 12 of I because of the revised value of ϕ (see Table XV). The renormalization group calculations of Aharony and Fisher[22] indicate that the position of the maximum is probably fairly accurate but its height relative to the critical point value should be appreciably greater (roughly 1% compared with 0.1%). The sharp falloff below T_c is exhibited quantitatively for the first time in this figure. However, the detailed precision immediately below the critical point (small $\Delta T/(ka)^{1/\nu}$) is also subject to the limitation that the expected $|t|^{1-\alpha}$ behavior has not been incorporated in the approximants. Significant effects of this defect will, however, be visible only on much enlarged scales. Since the $I(\vec{k}, T)$ versus T plots are monotonic below T_c the Ornstein-Zernike plots of $1/I(\vec{k}, T)$ versus k^2 will not cross one another for $T \leqslant T_c$ as they do above T_c (see I). However they will still exhibit the curvature that results from the nonzero value of η. Furthermore, insofar as the deviations from the Ornstein-Zernike form for $\hat{D}(x^2)$ are much larger below T_c than above, the deviations from linearity will be more marked.

C. Scattering approximants for two dimensions

In Sec. V C we did not develop a satisfactory approximant for representing the scattering intensity of the square lattice for general fields and temperatures. Above T_c the FB approximant (5.29) with $\phi = 0.02940$ and $\psi = 1.000108$ provides an excellent fit as shown in I.

On the *critical isotherm* the *ad hoc* approximant

$$\hat{D}_A(x^2) = \frac{(1+\phi'^2 x^2)^{\sigma+\eta/2}}{(1+\psi' x^2)(1+\phi''^2 x^2)^{\sigma}}, \tag{8.6}$$

introduced in (5.33), may be used with

$$\sigma = 2\eta, \quad \phi' = 0.3247, \quad \phi'' = 0.09355, \quad \psi = 1.0137. \tag{8.7}$$

This yields a fit to $\tilde{D}_\infty$ and to Σ_4^c (see Table VIII). The residual freedom has been removed by setting

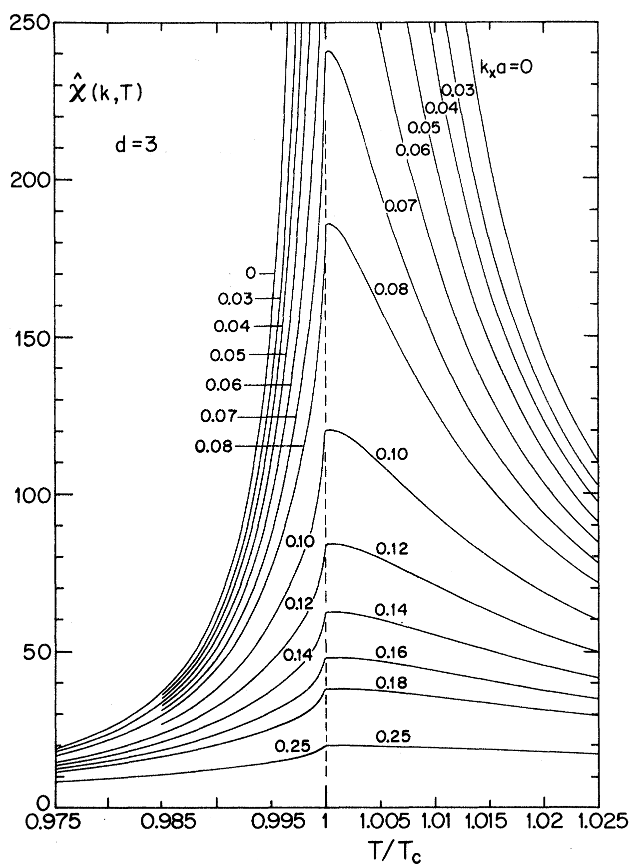

FIG. 5. Variation with temperature of the reduced scattering intensity $\hat{\chi}(\vec{k}, T) = I(\vec{k})/I_0(\vec{k})$ at fixed wave vector for three-dimensional lattices according to the asymptotic scaling expressions. The curves labelled by the values of $k_x a = k_y a = k_z a$.

$\phi'^2 = \frac{1}{4}\psi'$, which ensures that the second pair of singularities occurs at the expected two-particle branch points (relative to the single-particle poles at $x = \pm i\,|x_0|$). From the value of ψ follows the ratio f^c/f_1^c quoted in Table XIV. This deviates significantly from the mean-field value but great reliability cannot be placed in the precise value. The residual singularities in (8.6) are located, for the values (8.7), at $\pm 3.08i\,|x_0|$ and $\pm 10.69i\,|x_0|$. It is evident from Fig. 6, which is again a plot of the scaling function $\hat{D}(x^2)$ reduced by $\hat{D}_0(x^2)$, that the deviations from Ornstein-Zernike behavior exceed 10% even for x as small as 2.8. If suitable two-dimensional experimental systems can be found (e.g., absorbed submonolayers) such large deviations should be relatively easy to detect. (Note that the vertical scale in Fig. 6 is compressed by a factor of 4 relative to Fig. 4.)

On the *critical isochore below* T_c we adopt the approximant (5.45), namely,

$$\hat{D}_D^-(x^2) = \frac{(1 + \phi'^2 x^2)^{\eta/2}}{[1 - \lambda + \lambda(1 + \psi' x^2)^{1/2}]^2} \,. \tag{8.8}$$

As explained in Sec. V C, this exhibits the correct form of dominant square root branch points which, by choice of ψ', can be made to lie at the exactly known positions.[27-29] The normalization conditions and the fit to $\tilde{D}_\infty^c$ then lead to the parameter values

$$\phi' = 0.441, \quad \lambda = 0.3952, \quad \psi' = 2.592\,. \tag{8.9}$$

The consequent, exceptionally large value of the ratio $f^-/f_1^- = \psi'^{1/2}$ shown in Table XIV seems to be associated with the vanishing of the single-particle pole in the two-dimensional scattering intensity on the phase boundary (see Sec. V C). Regretably, the present calculations do not indicate how rapidly the ratio varies when a nonzero field is switched on. The second pair of singularities of the approximant (8.8), with (8.9), lie about 3.65 times further from the axis than do the dominant branch points.

As evident from Fig. 6 (which again supercedes the figure in Ref. 9) the deviations from Ornstein-Zernlike behavior are still larger below T_c than on the critical isotherm. Thus at $x \simeq 2$ the deviations already exceed 30%. The dotted curve in Fig. 6 is derived from the simple one-parameter approximant $\hat{D}_C(x^2)$ [defined in (5.42) and introduced in Ref. 9] which is fitted only to the value of $\tilde{D}_\infty^-$. The corresponding parameters $\lambda = 0.3933$ and $\psi' = 2.907$, lead to the rough estimate $f^-/f_1^- \simeq 1.705$. Comparison with the best estimate in Table XIV is most encouraging, considering the simplicity of this approximant.

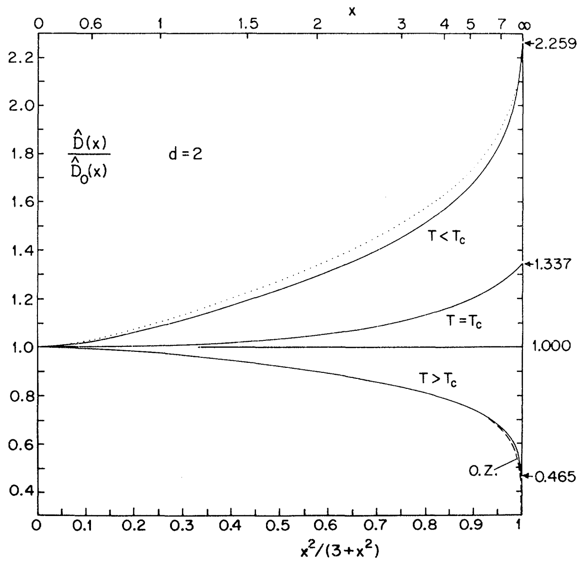

FIG. 6. Plots of the reduced scaling function approximants for two-dimensional lattices on the critical isochore ($T > T_c$), critical isotherm ($T = T_c$), and phase boundary ($T < T_c$). The dashed line represents the Ornstein-Zernike approximation. The dotted curve below T_c is calculated from the simpler, one-parameter approximant (5.41). Note the change of vertical scale relative to Fig. 4.

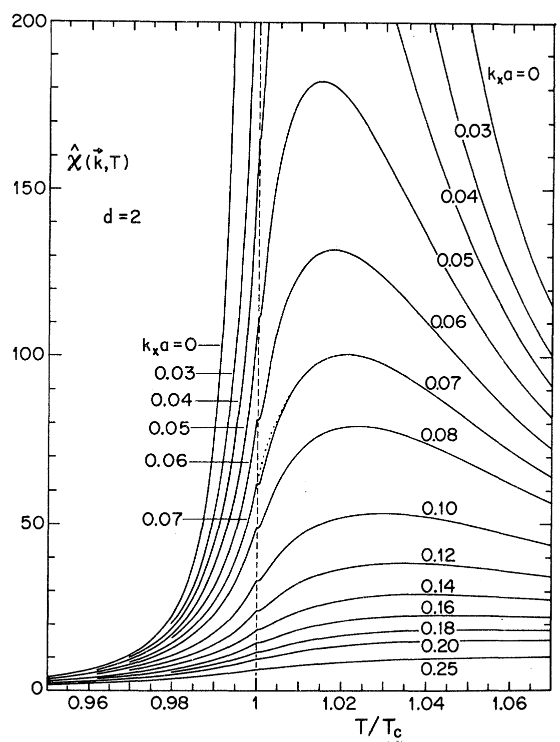

FIG. 7. Variation of the reduced scattering intensity with temperature for two-dimensional lattices according to the asymptotic scaling approximants at fixed $k_x a = k_y a$. Note that the small "shelf" just above T_c on each curve is an artifact of the approximant. The true behavior is indicated by the dotted curve on the plot for $k_x a = 0.07$.

TABLE XVI. Coefficients $c_{kl}(\vec{R})$ in the expansion of the inverse correlation function, $\mathcal{C}(\vec{R})$, in powers of u and y for the square lattice, where $\vec{R}=(x,y)a$ [see Eq. (6.2)].

k	l	(0, 0)	(1, 0)	(2, 0)	(1, 1)	(3, 0)	(2, 1)	(3, 1)	(2, 2)
0	0	0.25							
1	0	1.5	0.25						
1	1	−1	−0.25						
2	0	−0.25	0.5						
2	1	0	−1						
2	2	0.5	0.5						
3	0	3	−2	0	−0.25				
3	1	−6	5.5	0	1				
3	2	2	−5.5	0	−1.5				
3	3	2	2.5	0	1				
3	4	−1	−0.5	0	−0.25				
4	0	−19.75	9.5	0	1				
4	1	58	−29	0	−3				
4	2	−60.5	29.5	0	2				
4	3	28	−8	0	2				
4	4	−7.75	−4	0	−3				
4	5	2	2	0	1				
5	0	130	−52.5	0	−4.5	0	0		
5	1	−473	188.75	−0.5	13	0	−0.25		
5	2	654	−244.5	3	−5	0	1.5		
5	3	−421	117.75	−7.5	−21	0	−3.75		
5	4	126	13.5	10	31.5	0	5		
5	5	−23	−32.75	−7.5	−19	0	−3.75		
5	6	10	11.5	3	6	0	1.5		
5	7	−3	−1.75	−0.5	−1	0	−0.25		
6	0	−876.25	319	0	22.5	0	0		
6	1	3764	−1349	4	−71	0	2		
6	2	−6392	2210	−22	40	0	−11		
6	3	5298	−1685	48	98	0	24		
6	4	−2014.75	506.5	−50	−154	0	−25		
6	5	104	20	20	61	0	10		
6	6	162.5	0.5	6	22	0	3		
6	7	−54	−31	−8	−24	0	−4		
6	8	8.5	9	2	5.5	0	1		
7	0	6055	−2062	−0.75	−121.75	0	−0.5	0	−0.25
7	1	−29 972	10 088	−20.5	436	0	−9.25	0	2
7	2	60 590	−20 028	124	−374.5	−0.5	58	−0.25	−7.5
7	3	−63 018	20 290.5	−266	−423	4	−122	2	18
7	4	33 821	−10 609.5	231.5	916.25	−14	93	−7	−31.5
7	5	−6708	2440	25	−368	28	47.5	14	42
7	6	−1612	−301	−227	−317	−35	−152	−17.5	−42
7	7	1008	361	206	386	28	132	14	30
7	8	−206	−232	−92.75	−168	−14	−60.5	−7	−14.25
7	9	54	60.5	23.5	39	4	15.75	2	4
7	10	−12	−7.5	−3	−5	−0.5	−2	−0.25	−0.5

As stressed before, none of the closed-form approximants developed here gives a correct representation of the energy like singularity ($\sim t\ln|t|$ for $d=2$) to be expected in the scattering function at fixed wave vector as $T\rightarrow T_c$. In three dimensions this defect is not easily detected numerically unless a very large scale is used. However, in Fig. 7, which exhibits $I(\vec{k})/I_0(\vec{k})$ vs T according to (8.1) for fixed ka, the defect is apparent as a small "shelf" on the plots just at and above the critical point. This shelf is purely an artifact of our approximation procedures; the true variation should exhibit a vertical slope at the critical point as indicated roughly by the dotted portion of the plot for

TABLE XVII. Coefficients $c_{kl}(\vec{R})$ in the expansion of the inverse correlation function, $\mathcal{C}(\vec{R})$, in powers of u and y for the sc lattice, where $\vec{R}=(x,y,z)a$ [see Eq. (6.2)].

k	l	(0,0,0)	(1,0,0)	(2,0,0)	(1,1,0)	(3,0,0)	(2,1,0)	(1,1,1)	(3,1,0)	(2,1,1)	(2,2,0)
0	0	0.25									
1	0	2	0.25								
1	1	−1.5	−0.25								
2	0	−2	0.5								
2	1	3	−1								
2	2	−0.75	0.5								
3	0	17	−3.5	0	−0.25						
3	1	−39	10.5	0	1						
3	2	24	−11.5	0	−1.5						
3	3	1	5.5	0	1						
3	4	−3	−1	0	−0.25						
4	0	−156.75	28	0	2						
4	1	492	−100	0	−8						
4	2	−537	133.5	0	12						
4	3	213	−79	0	−8						
4	4	0.75	17.5	0	2						
4	5	−12	0	0	0						
5	0	1552	−260.5	0	−19	0	0	−0.75			
5	1	−6084	1108	−1	84	0	−0.25	3			
5	2	9066	−1839	6	−139.5	0	1.5	−2.25			
5	3	−6121	1440.5	−15	94	0	−3.75	−7.5			
5	4	1572	−451.5	20	4	0	5	18.75			
5	5	36	−50	−15	−42	0	−3.75	−18			
5	6	6	63	6	22.5	0	1.5	8.25			
5	7	−27	−10.5	−1	−4	0	−0.25	−1.5			
6	0	−16 205.5	2621.5	0	189.50	0	0	12			
6	1	76 011	−13 015	16	−937	0	4	−49.5			
6	2	−142 715.25	26 181.5	−100	1790	0	−25	39			
6	3	133 492	−26 622	264	−1490	0	66	132			
6	4	−60 825	13 263	−380	159	0	−95	−351			
6	5	8994	−1672	320	644	0	80	363			
6	6	1291.25	−1143	−156	−462	0	−39	−183			
6	7	120	398	40	106	0	10	36			
6	8	−148.5	−6	−4	3.5	0	−1	3			
6	9	−14	−6	0	−3	0	0	−1.5			
7	0	175 820	−27 757	−6.5	−1962.5	0	−2.5	−154.25	0	−1.25	−0.25
7	1	−959 454	158 035	−159	10 868	0	−34.75	697.5	0	8	2
7	2	2 170 128	−375 527	1228	−24 025	−1	295	−739.5	−0.25	−22	−7.5
7	3	−2 587 816	474 174	−3652	25 214	8	−892	−1532	2	38	18
7	4	1 683 453	−328 605.5	5825	−8909.25	−28	1409	5063.25	−7	−59.50	−31.5
7	5	−523 137	106 655.5	−5354	−6271	56	−1233.5	−5811	14	98	42
7	6	21 444	751.5	2654	6948.5	−70	506	3000	−17.50	−133	−42
7	7	20 115	−8269.5	−388	−1403	56	50	−204	14	122	30
7	8	−405	−266	−270.5	−861.25	−28	−150.5	−516.75	−7	−69.25	−14.25
7	9	226	941	145	462	8	62.25	225.5	2	22	4
7	10	−372	−131	−22	−60	−1	−9	−28.5	−0.25	−3	−0.5
7	11	0	0	0	0	0	0	0	0	0	0
7	12	−2	−1	0	−0.5	0	0	−0.25	0	0	0

$ka=0.07$. (This effect was not visible in the corresponding plots of I because of the smaller scale used there.) To correct the error one would have to undertake further study along the lines indicated in Sec. VIID where the strong scaling hypothesis was tested in just this domain.

Finally it should be noted that Fig. 6 and 4 represent only the asymptotic scaling form (8.1) but with $\chi_0(T)$ and $\xi_1(T,H)$ expressed through the representations presented in Appendix B. Owing to

TABLE XVIII. Coefficients $c_{kl}(\vec{R})$ in the expansion of the inverse correlation function, $\mathcal{C}(\vec{R})$, in powers of u and y for the bcc lattice, where $\vec{R}=3^{-1/2}(x,y,z)a$ [see Eq. (6.2)].

k	l	(0,0,0)	(1,1,1)	(2,2,2)	(2,0,0)	(2,2,0)	(3,1,1)	(3,3,1)
0	0	0.25						
1	0	2.5	0.25					
1	1	−2	−0.25					
2	0	−4.75	0.5					
2	1	8	−1					
2	2	−3	0.5					
3	0	44	−6.5	0	−1.5	−0.25		
3	1	−100	21.5	0	6	1		
3	2	56	−26.5	0	−9	−1.5		
3	3	12	14.5	0	6	1		
3	4	−12	−3	0	−1.5	−0.25		
4	0	−513.5	70	0	15	2.5		
4	1	1610	−266	0	−60	−10		
4	2	−1704	378	0	87	14.5		
4	3	572	−232	0	−48	−8		
4	4	80.5	39.5	0	−3	−0.5		
4	5	−30	15	0	12	2		
4	6	−15	−4.5	0	−3	−0.5		
5	0	6605.5	−845	0	−162.25	−27.75	0.25	0
5	1	−26 132	3712	−4.5	682	110	−6.25	−0.25
5	2	38 876	−6247	27	−979	−127	31.75	1.5
5	3	−25 548	4651.5	−67.5	302	−50	−73.25	−3.75
5	4	5943	−865.5	90	611.5	239	91.25	5
5	5	44	−766	−67.5	−670	−212	−62.75	−3.75
5	6	408	387	27	227	74	21.25	1.5
5	7	−156	−13.5	−4.5	−2	−4	−1.75	−0.25
5	8	−40.5	−13.5	0	−9.25	−2.25	−0.5	0
6	0	−90 127.5	11 056.5	0	1924	339.5	−5	0
6	1	428 334	−56 187	88.5	−8980	−1465	122	5
6	2	−808 872	114 027	−547.5	14 883	1880.5	−631	−31
6	3	749 312	−112 781	1410	−7048	674	1484	80
6	4	−325 320.5	48 053.5	−1920	−8061	−3986.5	−1858	−109
6	5	37 870	2332	1419	11 484	3814	1208	80
6	6	7525	−7399.5	−471	−4039	−1176.5	−262	−25
6	7	1356	69	−30	−792	−282	−124	−4
6	8	417	904.5	60	669	217	71	5
6	9	−368	−30	−7.5	−8	−5	−2	−1
6	10	−126	−45	−1.5	−32	−10	−3	0

the small ranges of $\Delta T/T_c$ and ka displayed, the corrections to the leading behavior will, however, be negligible on the graphical scale. Nevertheless, as mentioned above, greater accuracy away from the critical region can be obtained by replacing k by the effective wave vector $K(\vec{k})$.

ACKNOWLEDGMENTS

The support of the National Science Foundation, in part through the Materials Science Center at Cornell University, is gratefully acknowledged. The assistance of Professor K. G. Wilson in the computation of the series expansions is greatly appreciated. Dr. D. S. Gaunt kindly read and commented on the manuscript.

APPENDIX A: EXPANSION COEFFICIENTS

Values of the nonzero coefficients $c_{kl}(\vec{R})$ in the expansion (6.2) of the inverse correlation function, $\mathcal{C}(\vec{R})$, are given in Tables XVI–XVIII: all the numbers presented are exact. We quote the values on a set of topologically inequivalent sites. For a given lattice, $\mathcal{L}$, this is a minimal set of points $\{S\}$ such that the entire set of points of $\mathcal{L}$ can be generated by the group of homogeneous symmetry operations of $\mathcal{L}$ on $\{S\}$. From these data the cor-

TABLE XIX. Nonzero higher-order expansion coefficients $q_{kl}(\vec{R})$ of the correlation function $\Gamma(\vec{R})$ for the square lattice.

$\frac{1}{2}qk-l$	k	l	(0, 0)	(1, 0)	(2, 0)	(1, 1)	(3, 0)	(2, 1)	(4, 0)	(3, 1)	(2, 2)	(4, 1)	(3, 2)
4	8	12	36	24	12	16		8			4		
5	8	11	2592	1584	704	1136	192	512	16	128	192	8	32
5	9	13	1200	780	384	560	96	284	8	64	128	4	20
5	10	15	352	240	128	176	32	96		24	48		8
5	11	17	96	68	40	48	12	28		8	16		4

relation function $\Gamma(\vec{R})$ and specifically, the coefficients $q_{kl}(\vec{R})$ defined in (6.1) can be calculated completely for $k \leq 7$ on the sc and square lattices, and for $k \leq 6$ on the bcc lattices by using relation (2.8). However, the low-temperature grouping in powers of u is complete only up to $n = \frac{1}{2}qk - l = 3, 9$, and 14 for the square, sc, and bcc lattices, respectively. The additional nonzero coefficients $q_{kl}(\vec{R})$ needed to complete the low-temperature expansion for $\Gamma(\vec{R})$ up to order $n = \frac{1}{2}qk - l = 5, 12$, and 15, respectively, are listed in Tables XIX–XXI. These were evaluated directly using the techniques explained in Sec. VI B.

APPENDIX B: APPROXIMANTS FOR SUSCEPTIBILITY AND CORRELATION LENGTH

In this Appendix we record closed-form approximants for the reduced susceptibility or zero angle scattering intensity

$$\chi_0(H, T) = \mu_0(H, T) = \hat{\Gamma}(0, H, T), \tag{B1}$$

and for the squared second moment correlation length

$$[\xi_1(H, T)/a]^2 = \Lambda_2(H, T) = \mu_2(H, T)/2d\mu_0(H, T), \tag{B2}$$

(defined as in Sec. II), on the phase boundary below $T_c(H=0)$, and on the critical isotherm ($T = T_c$), for the square, sc, and bcc lattices.

As regards the *critical isochore* above $T_c(H=0)$, explicit approximants for $\ln(\kappa_1 a)^2 = -2\ln[\xi_1(T)/a]$ are given in Part I Eqs. (9.3), (9.4), (9.8), and Table V for square, triangular, sc, bcc, and fcc lattices. These expressions may be combined with Part I Eqs. (9.12), (9.13), and Table XX, which give explicit approximants for $\ln[r_1(T)/a]$, where $r_1(T)$ is the effective interaction range (which parameter has not been employed in this part). The reduced susceptibility may then be obtained from the relation (6.24) of I, namely,

$$\chi_0(H, T) = (\xi_1/r_1)^{2-\eta}, \tag{B3}$$

which, indeed, serves to define r_1 generally. Note that the modified ϕ_c estimates reported in II do *not* affect these results for ξ_1 and χ_0. However, these expressions do utilize the critical point estimates, (8.1) of I, namely,

$$\begin{aligned} v_c &= 0.218150 \quad u_c = 0.411950 \quad (\text{sc}), \\ &= 0.156172, \quad = 0.532676, \quad (\text{bcc}), \end{aligned} \tag{B4}$$

which differ from those adopted here[38c] [in (7.2) and (7.3)] by 9 parts in 10^5 and 2 parts in 10^4, respectively. For most practical purposes these differences will have little effect, if in particular, the values of v_c following from (7.2) and (7.3)[38c] are used in **(9.3) and (9.4) of I.** For $\chi_0(T)$ an alternative and more accurate procedure is to use approximants developed by Sykes, Gaunt, Roberts, and Wyles[38] [their Eqs. I (3.12) and II (3.18)(3.19)] whose critical point estimates we have adopted. Unfortunately, the approximants quoted in the published journal article are incorrect for the three-dimensional lattices. They were, however, corrected in the subsequent reprints and are restated here for convenience:

$$\begin{aligned} \chi_0(s) \simeq\ & 1.0161(1-s)^{-1.25} + 0.0590(1-s)^{-0.25} \\ & + 0.5610(1+s)^{0.875} + \Psi_{2,1}(s), \end{aligned} \tag{B5}$$

TABLE XX. Nonzero higher-order expansion coefficients $q_{kl}(\vec{R})$ of the correlation function $\Gamma(\vec{R})$ for the sc lattice.

$\frac{1}{2}qk-l$	k	l	(0, 0, 0)	(1, 0, 0)	(2, 0, 0)	(1, 1, 0)	(2, 1, 0)	(1, 1, 1)	(2, 1, 1)	(2, 2, 0)
11	8	13	864	416	32	224	16	120	8	
12	8	12	4508	1968	360	1016	168	560	80	4
12	9	15	960	480	64	256	32	144	16	

TABLE XXI. Nonzero higher-order expansion coefficients $q_{kl}(\vec{R})$ of the correlation function $\Gamma(\vec{R})$ for the bcc lattice.

$\frac{1}{2}qk-l$	k	l	(0, 0, 0)	(1, 1, 1)	(2, 2, 2)	(2, 0, 0)	(2, 2, 0)	(3, 1, 1)
15	7	13	2016	720	24	512	160	48

$$\Psi_{2,1}(s) = -0.6360 - 0.4669\, s + 0.0200\, s^2 - 0.0095\, s^3 - 0.0006\, s^4 - 0.0021\, s^5 - 0.0004\, s^6 - 0.0009\, s^7 - 0.0003\, s^8 - 0.0004\, s^9 - 0.0001\, s^{10} - 0.0002\, s^{11}, \tag{B6}$$

for the sc lattice, and

$$\chi_0(s) \simeq 0.9660(1-s)^{-1.25} + 0.1825(1-s)^{-0.25} + 0.5359(1+s)^{0.875} + \Psi_{2,1}(s), \tag{B7}$$

$$\Psi_{2,1}(s) = -0.6846 - 0.4732\, s - 0.0072\, s^2 - 0.0125\, s^3 - 0.0023\, s^4 - 0.0037\, s^5 - 0.0013\, s^6 - 0.0014\, s^7 - 0.0006\, s^8 - 0.0005\, s^9 - 0.0002\, s^{10} - 0.0001\, s^{11}, \tag{B8}$$

for the bcc lattice. We have defined

$$s = v/v_c = \tanh K/\tanh K_c. \tag{B9}$$

On the *phase boundary* below T_c we can write

$$\chi_0(T) \simeq u^{q/2}[X(u)]^\gamma/(u_c - u)^\gamma, \tag{B10}$$

where q is the coordination number, while the amplitude is represented by the Padé approximant

$$X(u) = \sum_{l=0}^{L} a_l u^l \Big/ \sum_{m=0}^{M} b_m u^m, \tag{B11}$$

which reproduces the exactly known coefficients of the low-temperature series and is consistent with the amplitudes given in Table I. The appropriate coefficients a_l and b_m are presented in Table XXII for sq, sc, and bcc lattices. Similarly we write

$$[\xi_1(T)/a]^2 = \Lambda_2(0, T) = u^{-1+q/2}[R(u)]^{2\nu}/(u_c - u)^{2\nu}, \tag{B12}$$

where the amplitude function is given by

$$R(u) = \sum_{l=0}^{L} p_l u^l \Big/ \sum_{m=0}^{M} q_m u^m. \tag{B13}$$

Suitable coefficients p_l and q_m are listed in Table XXIII.

On the *critical isotherm* ($T = T_c$) the susceptibility of the square lattice may be approximated by

$$\chi_0(H, T_c) \simeq \frac{0.1352y}{(1-y)^{14/15}} + X^c(y), \tag{B14}$$

while in three dimensions the form

$$\chi_0(H, T_c) \simeq \frac{X_0^c y}{(1-y)^{\gamma^c}} - \frac{X_1^c y}{(1-y)^{0.11}} + X^c(y), \tag{B15}$$

where $\gamma^c = \frac{4}{5}$ and

$$X_0^c = 0.4530,\quad X_1^c = 0.9340 \quad (\text{sc}),$$
$$= 0.4350,\quad = 0.6000 \quad (\text{bcc}), \tag{B16}$$

TABLE XXII. Nonzero coefficients a_l and b_m for the approximant $X(u)$ for the reduced susceptibility below T_c [see (B10) and (B12)].

	sq		sc		bcc	
l	a_l	b_l	a_l	b_l	a_l	b_l
0	0.378 864	1	0.411 985	1	0.532 789	1
1	−3.525 03	−8.047 22	−1.441 21	5.925 48	2.518 95	6.604 77
2	10.3562	17.4147	−1.146 49	1.999 92	5.267 34	22.2830
3	−10.6506	−3.654 42	−6.907 47	−34.2948	0.556 291	30.0673
4	3.641 34	−16.2533	−3.388 81	−29.8931	−11.4943	−11.2566
5		12.7754	16.7603	61.6797	−19.1338	−115.504
6			1.823 62	80.1663	−12.0624	−127.713
7			−9.696 46	−23.9523	−13.1656	−8.853 91
8			44.3908	−18.2269	57.6710	105.744
9					46.6145	78.4168
10					−163.979	4.769 68
11					−155.531	−7.792 16
12						−1466.08

TABLE XXIII. Nonzero coefficients p_l and q_m for the approximants $R(u)$ for the squared correlation length below T_c [see (B12) and (B13)].

	sq		sc		bcc	
l	p_l	q_l	p_l	q_l	p_l	q_l
0	0.171 573	1	0.411 985	1	0.666 393	1
1	7.720 67	46.3278	11.0636	30.0595	1.205 32	4.463 42
2	−10.705 46		30.6694	161.2060	3.645 94	15.9468
3	6.793 91		39.0192	351.3013	1.130 68	26.8846
4			16.6143	381.2285	10.5505	57.4373
5			−82.9380	30.4083	9.200 45	72.9269
6					−19.929 94	122.6957

while for each lattice $X^c(y)$ is a finite polynomial which is chosen to yield the correct values for the known expansion coefficients. Its coefficients, x_l, are listed in Table XXIV. The complex form of these expressions allows for the confluent critical singularities discussed in Secs. VII F and VII G.

TABLE XXIV. Nonzero coefficients x_l and e_l for the polynomials $X^c(y)$ and $E^c(y)$ entering the approximants for χ_0 and ξ_1^2 on the critical isotherm [see (B14) and (B19)].

	sq		sc		bcc	
l	x_l	e_l	x_l	e_l	x_l	e_l
1	−0.0175	0.0111	0.7607	0.0597	0.4693	0.0392
2	+0.0002	0.0088	0.0362	0.0004	0.0305	0.0000
3	−0.0118	0.0000	0.0056	0.0002	0.0031	−0.0010
4	−0.0017	0.0037	0.0050	−0.0003	0.0023	−0.0000
5	−0.0058	0.0038	0.0005	−0.0005	0.0000	−0.0007
6	−0.0013	0.0000	0.0005	−0.0001	0.0003	0.0002
7	−0.0043	−0.0003	0.0001	−0.0005	0.0000	
8	−0.0022		0.0002			

Similarly for the correlation lengths we may write for the square lattice

$$(\xi_1/a)^2 \simeq \Lambda_2(H, T_c) = \frac{0.1137y}{(1-y)^{16/15}} + \frac{0.0173y}{1-y} + E^c(y), \tag{B17}$$

while in three dimensions

$$(\xi_1/a)^2 \simeq \frac{F_0^c y}{(1-y)^{2\nu^c}} - \frac{F_1^c y}{(1-y)^{0.053}} - \frac{F_2^c y^2}{1-\frac{1}{2}y^2} + E^c(y), \tag{B18}$$

where $\nu^c = 72/175 = 0.4114\ldots$, and

$$\begin{aligned} F_0^c &= 0.1168, & F_1^c &= 0.0767, & F_2^c &= 0.0068 & &(\mathrm{sc}),\\ &= 0.1036, & &= 0.0486, & &= 0.0047 & &(\mathrm{bcc}), \end{aligned} \tag{B19}$$

Again, the functions $E^c(y)$ are polynomials whose coefficients, e_l, are also listed in Table XXIV.

*To whom reprint requests should be addressed.

[1]A. Münster, *Fluctuation Phenomena in Solids*, edited by R. E. Burgess (Academic, New York, 1965).
[2]Relevant reviews are: (a) M. E. Fisher, J. Math. Phys. 5, 944 (1964); (b) M. E. Fisher, Rept. Prog. Phys. 30, 615 (1967); (c) M. E. Fisher and D. Jasnow, The Theory of Correlations in the Critical Region (Academic, New York, to be published).
[3]The theory of neutron scattering is surveyed by W. Marshall and S. W. Lovesey, *The Theory of Thermal Neutron Scattering* (Oxford U. P., 1971).
[4]M. E. Fisher and R. J. Burford, Phys. Rev. 156, 583 (1967); note the corrections, etc., given in footnote 30 of Ref. 5. This is Part I.
[5]D. S. Ritchie and M. E. Fisher, Phys. Rev. B 5, 2668 (1972). This is Part II.
[6]L. S. Ornstein and F. Zernike, Proc. Acad. Sci. Amsterdam 17, 793 (1914); Z. Phys. 19, 134 (1918); 27, 761 (1926).
[7]D. Jasnow and M. Wortis, Phys. Rev. 176, 739 (1968).
[8]L. P. Kadanoff, Physics 2, 263 (1966).
[9]H. B. Tarko and M. E. Fisher, Phys. Rev. Lett. 31, 926 (1973). Note that there is a typographical error in the last column of Table I; correct values for the sq entries for $n = 7$ and 8 are given herein in Table X.
[10]D. S. Ritchie (private communication).
[11]See, e.g., R. Brout, *Phase Transitions* (Benjamin, New York, 1965).
[12]R. J. Elliott and W. Marshall, Rev. Mod. Phys. 30, 75 (1958).
[13]See H. B. Tarko, Ph.D. thesis (Cornell University, 1974).
[14](a) P. Schofield, Phys. Rev. Lett. 22, 606 (1969); (b) P. Schofield, J. D. Litster, and J. T. Ho, Phys. Rev. Lett. 23, 1098 (1969); (c) B. D. Josephson, J. Phys. C 2, 1113 (1969).
[15]M. E. Fisher in *Critical Phenomena, Proceedings of the 1970 Enrico Fermi International School, Course No. 51*, Varenna, Italy, edited by M. S. Green (Academic, New York, 1971), Sec. 3, p. 1.
[16]R. B. Griffiths, Phys. Rev. 158, 557 (1967); see also B. Widom, J. Chem. Phys. 41, 1633 (1964).

[17](a) D. S. Gaunt and C. Domb, J. Phys. C 3, 1442 (1970); (b) S. Milošević and H. E. Stanley, Phys. Rev. B 6, 986 (1972); 6, 1002 (1972); (c) R. Krasnow and H. E. Stanley, Phys. Rev. B 8, 332 (1973).

[18]P. G. Watson, J. Phys. C 2, 1883 (1969); 2, 2158 (1969); L. P. Kadanoff, Newport Beach Conference on Phase Transitions, Jan., 1970 (unpublished).

[19]E. Brézin, D. J. Wallace, and K. G. Wilson, Phys. Rev. Lett. 29, 591 (1972); Phys. Rev. B 7, 232 (1973); G. M. Avdeeva and A. A. Migdal, Zh. Eksp. Teor. Fiz. Pis'ma Red. 16, 253 (1972) [Sov. Phys.—JETP Lett. 16, 178 (1972)]; G. M. Avdeeva, Sov. Phys.—JETP 64, 741 (1973).

[20]J. W. Essam and D. L. Hunter, J. Phys. C 1, 392 (1968).

[21](a) G. W. Mulholland, Ph.D. thesis (Cornell University, 1973) (unpublished); (b) Gaunt and Domb (Ref. 17a) mentioned the possibility of using higher-order polynomials for $m(\theta)$; (c) The quintic model has also been considered by D. J. Wallace and R. K. P. Zia, Phys. Lett. A 46, 261 (1973).

[22]M. E. Fisher and A. Aharony, Phys. Rev. Lett. 31, 1238 (1973).

[23]See also (a) M. E. Fisher in *Critical Phenomena*, edited by M. S. Green and J. V. Sengers, NBS Misc. Publ. No. 273 (U.S. GPO, Washington, D.C., 1966), p. 108; (b) M. E. Fisher and J. S. Langer, Phys. Rev. Lett. 20, 665 (1968).

[24]General arguments can be based on the operator product expansion: L. P. Kadanoff, Phys. Rev. Lett. 23, 1430 (1969) and K. G. Wilson, Phys. Rev. 179, 1499 (1969); Phys. Rev. D 2, 1473 (1970).

[25]E. Brézin, D. Amit, and J. Zinn-Justin, Phys. Rev. Lett. 32, 151 (1974).

[26]W. J. Camp and M. E. Fisher, Phys. Rev. Lett. 26, 73 (1971); Phys. Rev. B 6, 946 (1972); M. E. Fisher and W. J. Camp, *ibid.* 6, 960 (1972); 7, 3187 (1973).

[27]T. T. Wu, Phys. Rev. 149, 380 (1966); H. Cheng and T. T. Wu, Phys. Rev. 164, 719 (1967).

[28]L. P. Kadanoff, Nuovo Cimento 44, B276 (1966).

[29]R. Hartwig and M. E. Fisher, Advan. Chem. Phys. 15, 333 (1969).

[30]C. Domb, Advan. Phys. 9, 149 (1960).

[31]R. Brout, Phys. Rev. 115, 824 (1959).

[32]G. Horowitz and H. Callen, Phys. Rev. 124, 1757 (1961).

[33]F. Englert, Phys. Rev. 129, 567 (1963).

[34]David Jasnow, Ph.D. thesis (University of Illinois, 1969) (unpublished); M. Wortis and D. Jasnow, Phys. Rev. 176, 739 (1968).

[35]K. G. Wilson (private communication).

[36]For a summary of the definitions we will use and some of the more important theorems in the theory of graphs the reader is referred to J. W. Essam and M. E. Fisher, Rev. Mod. Phys. 42, 272 (1970).

[37]In independent calculations for the fcc lattice, Dr. D. S. Ritchie has obtained six terms on the critical isotherm and 21 terms on the phase boundary (private communication). Adopting a smaller value of ν' than we do, he reports $f_1^+/f_1^- \simeq 1.93$. See also D. S. Ritchie and J. W. Essam (Westfield College, London, preprint) (to be published).

[38](a) M. F. Sykes, J. W. Essam, and D. S. Gaunt, J. Math. Phys. 6, 283 (1965); (b) M. F. Sykes, D. S. Gaunt, P. D. Roberts, and J. A. Wyles, J. Phys. A 5, 624 (1972); (c) J. Phys. A 5, 640 (1972).

[39]C. Domb and M. F. Sykes, J. Math. Phys. 2, 63 (1961).

[40]D. S. Gaunt and M. F. Sykes, J. Phys. A 6, 1517 (1973).

[41]D. S. Gaunt and M. F. Sykes, J. Phys. C 5, 1429 (1972).

[42]D. S. Gaunt, M. E. Fisher, M. F. Sykes, and J. W. Essam, Phys. Rev. Lett. 13, 713 (1964).

[43]M. A. Moore, D. M. Jasnow, and M. Wortis, Phys. Rev. Lett. 22, 940 (1969).

[44]M. Ferer and M. Wortis, Phys. Rev. B 6, 3426 (1972).

[45]For a recent survey of series extrapolation procedures including Padé approximant techniques see D. L. Hunter and G. A. Baker, Jr., Phys. Rev. B 7, 3346 (1973); 7, 3377 (1973).

[46]E. Barouch, B. M. McCoy, and T. T. Wu, Phys. Rev. Lett. 31, 1409 (1973).

[47]J. W. Essam and M. E. Fisher, J. Chem. Phys. 38, 802 (1963).

[48]M. Ferer, M. A. Moore, and M. Wortis, Phys. Rev. Lett. 22, 1382 (1969).

[49]M. E. Fisher and H. B. Tarko, Phys. Rev. B (to be published).

[50]H. Garelick and J. W. Essam, J. Phys. C 1, 1588 (1968); P. E. Scesney, Phys. Rev. B 1, 2274 (1970).

[51]D. S. Gaunt, Proc. Phys. Soc. 92, 150 (1967).